

# Physically Based Modelling for Knock Prediction in SI Engines

**Nils Thornberg and Jonas Eriksson Kraft**

Master of Science Thesis in Electrical Engineering  
**Physically Based Modelling for Knock Prediction in SI Engines**

Nils Thornberg and Jonas Eriksson Kraft  
LiTH-ISY-EX--18/5136--SE

Supervisor: **Assistant Professor Andreas Thomasson**  
ISY, Linköping University  
**Ph.D Student Xavier Llamas Comellas**  
ISY, Linköping University  
**Olaf Eickel and Henrik Voss**  
Volvo Cars

Examiner: **Professor Lars Eriksson**  
ISY, Linköping University

*Division of Automatic Control  
Department of Electrical Engineering  
Linköping University  
SE-581 83 Linköping, Sweden*

Copyright © 2018 Nils Thornberg and Jonas Eriksson Kraft

## **Abstract**

The high demand for an increase in performance and at the same time lowering the emissions is forcing the automotive industry to increase the efficiency of the vehicles. This demand lead to a problem called knock, which often is the limiting factor when increasing the efficiency of the engine. Knock occurs when the unburned gases inside the combustion chamber self-ignites due to the increasing pressure and temperature.

This thesis investigates if it is possible to predict knock with a physically based knock model. The model consist of several sub-models such as pressure model, temperature model and knock model. The models are built by using measured data and the goal is to get an independent knock prediction model that can find the limited ignition angle that will cause knock.

The results shows that an analytic pressure model can simulate a measured pressure curve. But when it comes to predicting knock, there is an uncertainty which can be improved by changing the modelling strategy and making the models more accurate.



## **Acknowledgments**

We would like to thank Volvo Cars and our examiner, Lars Eriksson, for the opportunity to write this thesis. Also, a big thanks to our supervisors at Volvo Cars, Olaf Eickel and Henrik Voss, and our supervisors here at Linköping University, Xavier Llamas Comellas and Andreas Thomasson, for their support and guidance throughout the whole master thesis.

We would also like to thank all the other Master thesis students at our office for all the interesting discussions and funny moments that kept us motivated during the thesis.

*Linköping, June 2018*  
*Nils Thornberg and Jonas Eriksson Kraft*



---

# Contents

<b>Notation</b>	<b>ix</b>
<b>1 Introduction</b>	<b>1</b>
1.1 Problem formulation . . . . .	1
1.2 Purpose and goals . . . . .	2
1.3 Expected results . . . . .	2
1.4 Outline . . . . .	2
<b>2 Related research</b>	<b>5</b>
2.1 Knock . . . . .	5
2.1.1 Knock control strategy . . . . .	6
2.2 Combustion . . . . .	7
2.3 Octane number . . . . .	8
2.4 EGR . . . . .	8
<b>3 Modelling</b>	<b>11</b>
3.1 Knock model . . . . .	12
3.2 Temperature model . . . . .	12
3.3 Heat release analysis . . . . .	14
3.3.1 Combustion model via the Vibe function . . . . .	15
3.4 Pressure at IVC . . . . .	16
3.5 Gatowski . . . . .	16
3.5.1 Heat release rate . . . . .	17
3.5.2 Heat Transfer . . . . .	18
3.5.3 Specific heat ratio . . . . .	18
3.5.4 Crevice model . . . . .	20
3.6 Analytic cylinder pressure Model . . . . .	20
3.6.1 Compression Asymptote . . . . .	20
3.6.2 Expansion Asymptote . . . . .	21
3.6.3 Combustion . . . . .	22
3.6.4 Gas exchange . . . . .	22
3.6.5 Complete pressure model . . . . .	22
3.7 Summary of the in-cylinder models . . . . .	23

3.8	Polynomial models for the combustion parameters . . . . .	24
3.9	Knock prediction model . . . . .	25
3.9.1	Knock onset algorithm . . . . .	25
<b>4</b>	<b>Data processing</b>	<b>29</b>
4.1	Data description . . . . .	29
4.1.1	Engine data . . . . .	29
4.1.2	Measured data . . . . .	30
4.2	Pressure pegging . . . . .	30
4.3	Filter the measurement signal . . . . .	32
4.4	Knock onset . . . . .	32
4.4.1	Tuning the coefficients in the knock model . . . . .	34
<b>5</b>	<b>Result and discussion</b>	<b>35</b>
5.1	Knock onset . . . . .	35
5.1.1	Tuning the knock model . . . . .	37
5.2	Unburned Temperatures . . . . .	39
5.3	Heat release analysis and mass fraction burned . . . . .	39
5.4	Pressure at IVC . . . . .	40
5.5	Pressure model . . . . .	41
5.5.1	Gatowski model . . . . .	41
5.5.2	Analytical model . . . . .	43
5.5.3	Simulated knock onset for both pressure models . . . . .	45
5.5.4	Polynomial models . . . . .	47
5.5.5	Pressure validation with the polynomial models . . . . .	50
5.5.6	Knock onset validation with polynomial models . . . . .	53
5.6	Knock prediction model . . . . .	55
5.6.1	Knock onset algorithm . . . . .	56
5.7	Discussion . . . . .	57
<b>6</b>	<b>Conclusion</b>	<b>59</b>
6.1	Future work . . . . .	60
<b>A</b>	<b>Polynomial values</b>	<b>63</b>
	<b>Bibliography</b>	<b>65</b>

---

# Notation

## ABBREVIATIONS

---

<b>Abbreviations</b>	<b>Description</b>
ABDC	After Bottom Dead Center
ATDC	After Top Dead Center
BDC	Bottom Dead Center
CA	Crank angle
CPU	Central Processing Unit
DBL	Detonation Border Line
ECU	Engine Control Unit
EM	Exhaust manifold
EGR	Exhaust Gas Recirculation
EOC	End Of Combustion
EVO	Exhaust Valve Open
FFT	Fast Fourier Transform
IM	Intake Manifold
IVC	Intake Valve Closing
MBT	Maximum Brake Torque
MFB	Mass Fraction Burned
ON	Octane Number or Octane Rating
PPP	Position of Peak Pressure
SI	Spark Ignition
SOC	Start Of Combustion
TDC	Top Dead Center

---



# 1

---

## Introduction

### 1.1 Problem formulation

The demand for higher performance and continuously stricter emissions regulations is pushing the automotive manufacturers to increase the efficiency of the vehicles. The development towards smaller engines that fulfills these demands causes the problem called knock.

Knock is often the limiting factor when trying to increase the efficiency of the engine via combustion phasing. Knock occurs when the air/fuel-mixture in front of the ordered flame self-ignites. This creates a high local pressure wave that can damage the engine. It can be avoided by retarding the ignition angle, but this decreases the output power of the engine. Therefore, the trade-off between a higher engine power output and a suitable durability of the engine components is a challenging task for the manufacturers.

Today, most manufacturers use a control strategy for the ignition angle that is based on a rough estimation of where knock will occur. This estimation is based on experiments on different operating points and uses different compensating factors based on EGR, temperature and other driving conditions. This method is just a rough guess and the real knock limit may in some cases be far from the one estimated, if the engine operates far from nominal conditions. The engines are equipped with an accelerometer sensor which is detecting knock based on the vibrations created from the knock event.

It is desirable to be able to predict the knock limit angle using a physically based model. An accurate physical model of the knock limit would make the knock limit controller more trustworthy, which in turn could lead to a more efficient ignition timings. Potentially, the tuning requirements of a physical model could be lower and the calibration time for a specific engine could decrease.

## 1.2 Purpose and goals

The purpose of the thesis is to investigate the knock phenomena on a Volvo four stroke SI engine. One objective is to research what engine parameters that affect the knock ignition limit the most.

The main goal is to develop physical based model for predicting knock onset. The model should handle several input parameters like temperature, pressure, internal and external EGR, engine speed, cam phasing, fuels with a different octane number, water injection, etc. The model will be developed using Matlab, and the calculations should be kept easy to minimize the CPU load. Low CPU usage increases the possibility to use the model in real time in an Engine control unit (ECU).

The following are carried out in this thesis:

- Build a in-cylinder pressure model that can simulate a measured pressure trace.
- Investigate if a physically based model can determine if knock will appear
- Determine which engine parameters that are strongly connected to knock tendency

## 1.3 Expected results

The expected result of this thesis is to develop a physical based knock model that can predict when knock will occur. The model will be developed using measurements from the test engine. The final model will then be validated by comparing the predictions to the experimental data.

## 1.4 Outline

This thesis consist of 5 chapters and a short description of each chapter can be seen below.

- **Chapter 1 - Introduction**  
Presents the problem formulation, the purpose and the goals of the thesis.
- **Chapter 2 - Related research**  
Presents related research about topics covered in the thesis.
- **Chapter 3 - Modelling**  
This chapter describes how the thesis goals are pursued. All the models and equations that are required to reach the goal are presented.
- **Chapter 4 - Data processing**  
Presents the experimental setup and how the data was processed.

- **Chapter 5 - Result and discussion**

In this chapter the result of the developed model will be validated with real engine data. The results will be discussed throughout the whole chapter.

- **Chapter 6 - Conclusion and future work**

In this chapter the conclusion of the results are discussed and the questions in the problem formulation are answered.



# 2

---

## Related research

### 2.1 Knock

Normal combustion is triggered when the gases inside the combustion chamber are ignited by a spark. Sometimes an abnormal combustion occurs and this phenomena is called knock.

Knock occurs when the unburned gases in front of the developed flame self ignites. The self ignition is due to the increased pressure and temperature that is created when the flame front is moving inside the cylinder. This will produce high local pressures as well as pressure waves inside the combustion chamber, see figure 2.1 for an illustration. Sustained knock in the engine can cause severe damage inside the cylinders. It also makes a loud and irritating noise which can be a distraction for the operator of the vehicle, see Heywood [12] for more information.

A common way of avoiding knock in SI engines is to retard the ignition timing, see Lezium et al. [20]. This will lead to a lower knock probability since the pressure in the cylinder will decrease. The trade-off between low knock probability and high engine output power is a big challenge when designing the controller.

Knock can be detected in several different ways based on what instruments that are used. While developing and analyzing engines, a common way is by looking at the in cylinder pressure curve. By using a high pass filter on the pressure curve, the knock intensity as well as the knock duration can be determined based on the pressure peak and the duration of the pressure oscillations, see Jong-Hwa Lee and Jin-Soo Lim [15] and Lezium et al. [20]. Another way to detect knock is by measuring the ion-current in the cylinder as in Eriksson [4]. When combustion occurs in the cylinder, ions are released which builds an ion-current in the cylinder. This current can then be measured with the spark plug placed inside the cylinder. When knock occurs, it can be detected since the ion-current

in the cylinder will oscillate and have a similar behavior as the pressure during knock, see Eriksson [4] and Kinoshita et al. [17] for practical applications. Knock can also be detected by studying the frequencies of the vibrations. These vibrations are developed by the oscillating pressure in the cylinder. The frequencies is transferred to the engine block and can then be captured by accelerometers which are placed on the engine block. This is a very common method in production engines since it is very cost effective and it does not require expensive pressure sensors inside the cylinder. The downside with this method is that other vibrations interfere with the accelerometers as described in Scholl et al. [22] and Chang et al. [2].

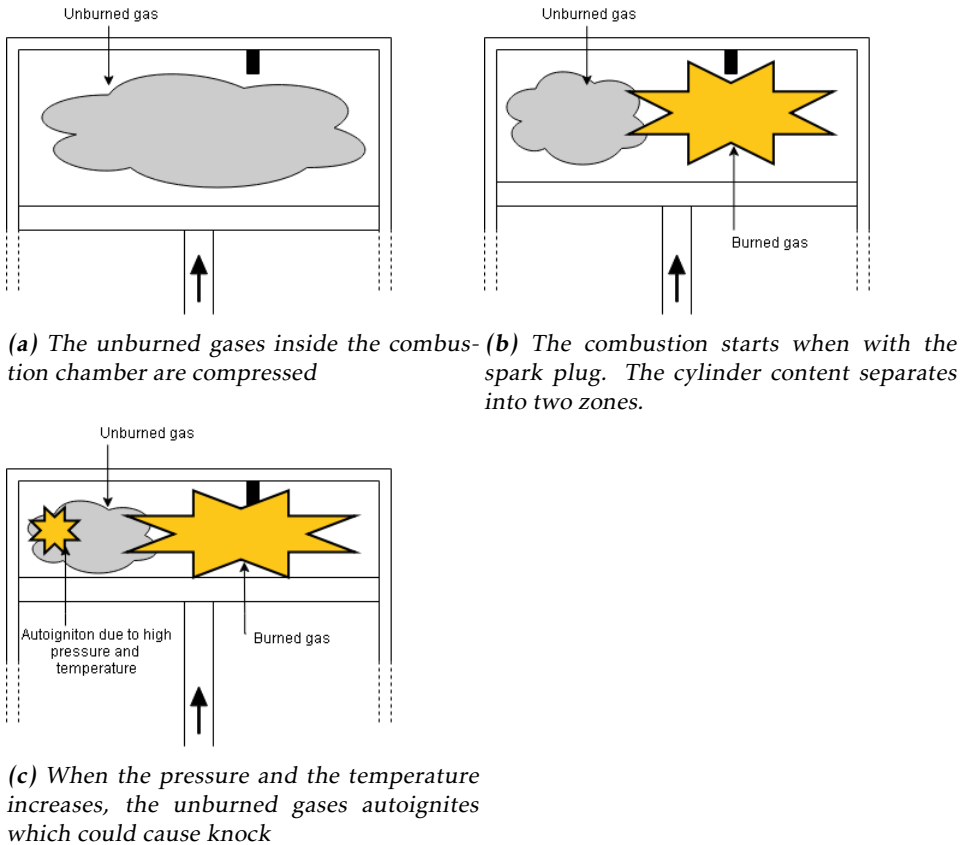


**Figure 2.1:** Shows the combustion process inside the cylinder

### 2.1.1 Knock control strategy

While controlling knock, the conventional strategy differs from regular control algorithms. Regular control algorithms usually have a reference value which the controller tries to hold as close as possible. In the case of conventional knock

controllers, this control strategy does not work since continued knock can cause severe damage to the engine. Therefore, in an event of knock, the controller takes immediate action and retards the ignition a fixed amount for each cycle until a cycle without knock is detected. Every cycle without knock, the controller advances the spark until knock occurs. See Kiencke and Nielsen [16] and Thomasson et al. [23] for more information.

In Thomasson et al. [24] a different knock control strategy is investigated, which is a likelihood-based strategy. As the conventional control strategy, this is also an event based strategy. The main difference is that this controller only adjust the spark timing if there is statistical evidence that the knock probability is above a given threshold.

## 2.2 Combustion

When analyzing knock in the engine, it is important to understand the combustion process. In an SI engine, the combustion is initiated by the spark plug. The timing when the spark plug ignites the mixture is crucial for the pressure curve in the cylinder. An early spark ignition usually yields higher maximum temperature and maximum pressures at earlier crank angles, which can decrease the efficiency of the engine due to a too early pressure build up that counteracts the piston movement. A similar outcome occurs if the ignition is too late since the pressure increase from the combustion is developed too late in the expansion phase [4]. In Eriksson and Andersson [5], an analytic model of the cylinder pressure was developed and validated. The model could trace the pressure during the combustion and the expansion with a good accuracy and at the same time having a low computational demand.

The optimal ignition angle is the ignition timing that results in the maximum generated power and thus the best engine efficiency. This angle is named maximum brake torque (MBT). As mentioned in Hubbard et al. [14], Heywood [12] and Zhu et al. [27], MBT is usually defined as the angle that places the position of the peak pressure (PPP) around 15-16° ATDC. Another way of defining the MBT is discussed in Eriksson [4], where it is defined as the angle that places the 50% of the mass fraction burned (MFB50) at 8-10° ATDC. The ignition timing which is the breakpoint for when knock will occur is called detonation border line (DBL). Sometimes the MBT angle is located before the DBL. In this case knock will occur if the ignition angle follows the MBT. In these operating points it is better to delay the spark timing to avoid knock and possible damage to the cylinders. Therefore, the ignition angle is set to be as follows

$$\theta_{ign} = \min(MBT, DBL) \quad (2.1)$$

The in-cylinder thermodynamic process can be modelled in different ways as discussed in Yeliana et al. [26]. The paper compares a single zone model with a two-zone model. A single zone heat release model treats the content in the cylinder as a uniform gas. The two-zone model divides the content into two distinct zones - the burned and the unburned. The conclusion was that both

models are accurate when analyzing the mass fraction burned ( $X_b$ ), but the two-zone model is preferred when a more detailed in-cylinder temperature is desired. Several other researches have investigated the two-zone model when modelling knock in engines [8, 9, 11, 21]. The results showed that the two-zone model were able to predict the cylinder temperature with good accuracy.

When tracing the mass fraction burned during the combustion the well known Vibe function is often used. The Vibe function requires information about the ignition, such as the crank angle when the spark ignites, the flame development angle and the rapid burned angle. More information about function can be found in Vibe [25]. In Elmqvist et al. [3], the Vibe function was used in a knock prediction model. The model could predict knock within a few crank angle degrees which was considered as a very good result.

## 2.3 Octane number

The fuel used in SI-engines consists of blends of different hydrocarbons. The characteristics of the fuel and the ability to self ignite will depend on what kind of hydrocarbons are included in the blend. The octane number, also called *ON* or octane rating, is a measure of the fuels resistance to self ignite and cause knock. A blend with a high octane number is more resistant to knock than a blend with a low octane number. The number is defined as the mixture between heptane and isooctane which are two hydrocarbons. Those two hydrocarbons were chosen because of the different ability to self ignite and cause knock. Heptane has a high sensitivity to knock and isooctane is very knock resistant. If a blend consists of 90 % isooctane and 10 % heptane, then the octane number will be 90. More information can be found in Heywood [12].

## 2.4 EGR

Exhaust gas recirculation (EGR) is a technique used in combustion engines to reduce the  $NO_x$  emissions. The purpose of this technique is to recycle some of the burned gases from the exhaust manifold to the intake manifold. The burned gas is cooled and mixed with new fresh air which increase the specific heat capacity of the mixture in the cylinder. This will lower the burning temperature during the combustion. According to Kiwan et al. [18], these characteristics will contribute to a lower peak in-cylinder temperature during combustion and a decrease in  $NO_x$  emission since it is very temperature dependent. One more advantage with EGR is that it can lower the part load fuel consumption cause it increases the pressure in the intake manifold which reduces the pumping work. Also by using a cooled EGR, the combustion can be more tolerant to knock. A downside with EGR is that it increases the variations from cycle to cycle, which can be seen in Eriksson and Nielsen [6].

Tests have been done using EGR on boosted direct-injected SI engine in Hoepke et al. [13] as well as the effects of combined external and internal EGR in Cairns

---

and Blaxill [1]. Both studies showed that the EGR was able to extend the knock limit which resulted in higher peak load and more fuel efficiency.



# 3

## Modelling

This chapter will cover the modelling approach that was chosen for modelling the knock onset, heat release, in-cylinder pressure, temperature and finally the unburned temperature of the cylinder content. To get a better understanding of what models that are used and overview of the modelling strategy is presented in figure 3.1.

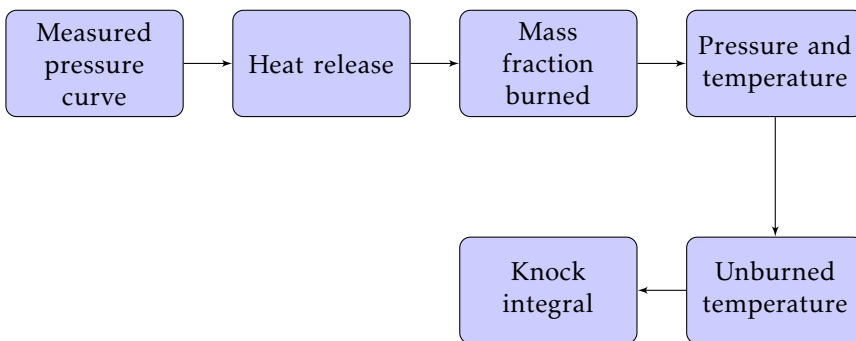


*Figure 3.1: An overview of the modelling approach*

The overview describes how the knock will be modelled and what submodels that are needed. From the measured pressure curve, the heat release is calculated. The heat release is closely connected to the mass fraction burned (MFB) and from the MFB the start of combustion (SOC) is determined. When the SOC is known, the combustion process is modelled with a Vibe function which later can be used in the pressure model and the temperature model. The design parameters in the pressure model are optimized so the error between the measured pressure and the model pressure is as small as possible. Thereafter, the unburned temperature

is modelled and used in the knock integral that determines if there is knock or not.

To get a better understanding of what parameters that are important when modelling, each submodel will be explained in detail later in this chapter. Two different pressure models are presented, one model calculates the pressure with a differential equation and the other is an analytic model which is less computational demanding.

### 3.1 Knock model

The goal with the knock model is to examine if the engine is knocking or not at a certain operation condition. To be able to track when knock is about to occur, it is necessary to know the temperature and pressure at the unburned zone. This requires submodels for the pressure and temperature that are implemented into the knock model.

The knock model is built on the knock integral and is shown in equation (3.1) where  $\tau$  is the ignition time delay, see Heywood [12].

$$KI(\theta) = \int_{\theta_{ivc}}^{\theta} \frac{1}{\tau} d\theta \quad (3.1)$$

The ignition time delay is based on the Arrhenius function. This function is shown in equation (3.2) and is based on the unburned temperature  $T_u$  and the cylinder pressure  $p$ . This equation also includes the constants  $X_1$ ,  $X_2$  and  $X_3$  as in Elmqvist et al. [3].

$$\tau = X_1 \cdot p^{-X_2} \cdot e^{\frac{X_3}{T_u}} \quad (3.2)$$

This model is often tuned so the  $KI(\theta_{knock})$  is equal to one when knock occur. This timing is called knock onset and describes at which crank angle knock will occur. This is done by tuning the constants  $X_1$ ,  $X_2$  and  $X_3$  with the experimental data. As mention in Elmqvist et al. [3], a general rule is that the engine is safe from knock if  $KI < 1$  for  $x_b < 0.93$  because there is no mass left to cause damage if knock occurs after that point. In Heywood [12] and Eriksson and Sivertsson [8], the constants were tuned as the equation (3.3) which will be used as a starting point, and later optimized to fit the measured data.

$$\tau = 0.01768 \left( \frac{ON}{100} \right)^{3.402} p^{1.7} e^{\frac{3800}{T_u}} \quad (3.3)$$

### 3.2 Temperature model

As seen in the knock model, the temperature of interest is the unburned end gases temperature. The model for this is described in Eriksson and Sivertsson [8] where a single zone model is extended to a semi two-zoned model.

The single zone model for the temperature is based on ideal gas law as

$$pV = mRT \quad (3.4)$$

where the total mass charge ( $m$ ) and the specific gas constant ( $R$ ) is assumed to be constant. The relationship between two point can then be defined as

$$\frac{p_i v_i}{T_i} = \frac{p_{i+1} v_{i+1}}{T_{i+1}} \quad (3.5)$$

Since the volume and the pressure is known during the whole cycle, one can take a reference value, like the inlet valve closing time (IVC), and get the following expression for the cylinder temperature

$$T(\theta) = \frac{T_{IVC}}{p_{IVC} V_{IVC}} p(\theta) V(\theta) \quad (3.6)$$

The two zone model divide the content in the cylinder into two zones - the burned and the unburned temperature of the air and fuel mixture. By using this model, the zones can be separated and properties of the content in the cylinder can be more accurate. The two zone model divide the four stroke cycle in three phases. The first phase is IVC to SOC where the content in the cylinder is seen as one zone - the unburned. The second phase is SOC to EOC, in this phase there is an unburned zone and a burned zone. The three following temperatures can be tracked during this phase, cylinder average temperature ( $T$ ), unburned gas temperature ( $T_u$ ) and the burned gas temperature ( $T_b$ ). The third phase is EOC to EVO, in this phase there is only one phase - the burned. As mention before, the temperature of interest is only the unburned temperature and thereby only the second phase. The compression is assumed to be adiabatic process and the relationship between two point can then be defined as

$$p_i V_i^\gamma = p_{i+1} V_{i+1}^\gamma \iff \frac{p_i}{p_{i+1}} = \left( \frac{V_{i+1}}{V_i} \right)^\gamma \quad (3.7)$$

Equation (3.7) combined with the ideal gas law, equation (3.5), gives the following relationship,

$$\frac{p_i V_i}{T_i} = \frac{p_{i+1} V_{i+1}}{T_{i+1}} \iff \frac{T_{i+1}}{T_i} = \frac{p_{i+1} V_{i+1}}{p_i V_i} = \frac{p_{i+1}}{p_i} \left( \frac{p_i}{p_{i+1}} \right)^{\frac{1}{\gamma}} = \left( \frac{p_{i+1}}{p_i} \right)^{\frac{\gamma-1}{\gamma}} \quad (3.8)$$

Again, the IVC is used as a reference point to calculate the temperature at SOC as

$$T_{u,SOC} = \frac{T_{IVC}}{p_{IVC} V_{IVC}} p_{SOC} V_{SOC} \quad (3.9)$$

The unburned temperature is modelled with equation (3.8) with the SOC as the reference value

$$T_u(\theta) = T_{u,SOC} \left( \frac{p(\theta)}{p_{SOC}} \right)^{\frac{\gamma-1}{\gamma}} \quad (3.10)$$

The final expression for the unburned temperature is stated below,

$$T_u(\theta) = \begin{cases} \frac{T_{IVC}}{p_{IVC}V_{IVC}} p(\theta)V(\theta) & \text{if } \theta \leq \theta_{SOC} \\ T_{u,SOC} \left( \frac{p(\theta)}{p_{SOC}} \right)^{\frac{\gamma-1}{\gamma}} & \text{if } \theta > \theta_{SOC} \end{cases} \quad (3.11)$$

where the specific heat ratio ( $\gamma$ ) is the modified linear model presented in section 3.5.3.

### 3.3 Heat release analysis

The heat release analysis is done on the measured pressure curve and the modelled temperature according to equation (3.6). The goal of this analysis is to estimate the MFB trace during the combustion. The heat release model is based on the first law of thermodynamics where the pressure trace, volume change and the cylinder content is known.

The heat release equation is stated as

$$dQ_{ch} = dU + dW \quad (3.12)$$

where the change in energy due to combustion ( $dQ_{ch}$ ) is equal to the change in internal energy ( $dU$ ) and the work done in the system ( $dW$ ). This model treats the cylinder content as one unit. The change in internal energy is stated as

$$dU = mc_v dT \quad (3.13)$$

where  $m$  is the charge mass calculated with the ideal gas law and  $c_v$  is the specific heat. The change in temperature ( $dT$ ) is determined with the ideal gas law and is stated as

$$dT = \frac{1}{mR} (pdV + VdP) \quad (3.14)$$

With equation (3.12) - (3.14) and the piston work written as  $dW = p dv$ , the final expression for the heat release is stated as

$$dQ_{ch} = mc_v \frac{1}{mR} (pdV + VdP) + pdV \quad (3.15)$$

MFB is assumed to be proportional to the released energy (heat) in the system. Hence, the MFB can be expressed as a function of the heat released as in equation (3.16).

$$x_b(\theta) = Q_{ch}(\theta)/\max(Q_{ch}) \quad (3.16)$$

From the MFB curve the SOC, end of combustion (EOC) and the combustion duration ( $\Delta\theta$ ) is approximated. The downside with this method is that no losses are taken into account when calculating the amount heat released. But according to Heywood [12], the exclusion of the losses does not affect the shape of the heat release much and will therefore not affect the shape of the mass fraction burned.

### 3.3.1 Combustion model via the Vibe function

Another way of describing the combustion process and the MFB is the well known vibe function. The vibe function can be used to simulate the combustion process by fitting the curve to the MFB trace received from heat release analysis. Hence, the vibe function is dependent of an already known pressure trace and can therefore never be used in a predictive model, only a semi-predictive model which is discussed in Elmqvist et al. [3]. The vibe function is stated in Eriksson and Nielsen [6] as

$$x_b(\theta) = \begin{cases} 0 & \theta < \theta_{ign} \\ 1 - e^{-a\left(\frac{\theta - \theta_{ign}}{\Delta\theta}\right)^{m+1}} & \theta \geq \theta_{ign} \end{cases} \quad (3.17)$$

where  $x_b(\theta)$  is the MFB,  $\Delta\theta$  and  $a$  are combustion duration parameters and  $m$  defines the shape of the burning profile. The approximation of  $a$  and  $m$  is described in Eriksson [4] as

$$m = \frac{\ln\left(\frac{\ln(1-0.1)}{\ln(1-0.85)}\right)}{\ln(\Delta\theta_d - \ln(\Delta\theta_d) + \Delta\theta_b)} - 1 \quad (3.18)$$

$$a = -\ln(1 - 0.1) \left(\frac{\theta}{\Delta\theta_d}\right)^{m+1} \quad (3.19)$$

where  $\Delta\theta_b$  is the rapid burn angle which describes the crank angle between 10-85 % MFB and  $\Delta\theta_d$  is the flame development angle which describes the crank angle between 0-10 % MFB. Due to the overparameterization, either  $a$  or  $\Delta\theta$  needs to be specified to get a solution. The following expression is a common approximation of the combustion duration

$$\Delta\theta = 2\Delta\theta_d + \Delta\theta_b \quad (3.20)$$

The Vibe parameters can be solved with *lsqnonlin* which is a non linear least square solver in Matlab. The goal is to minimize the error between the MFB from the heat release and the Vibe function curve. A typical shape of the vibe function can be seen in figure 3.2 where the rapid burn angle and flame development angle are marked in the plot.

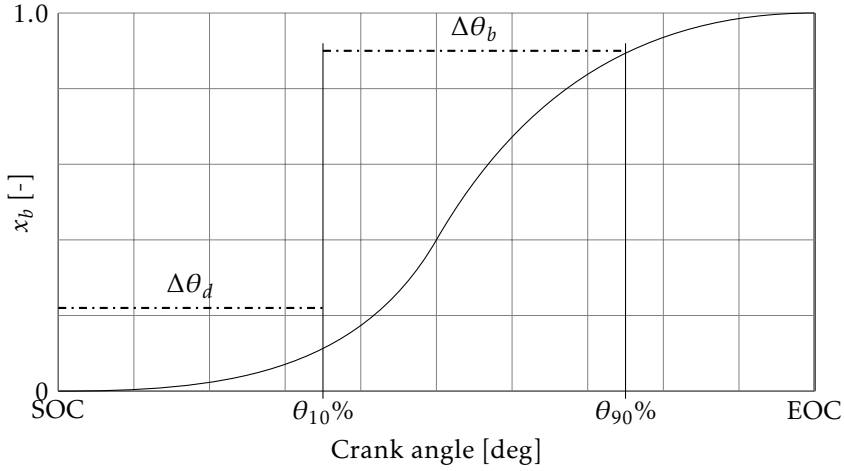


**Figure 3.2:** The shape of the Vibe function where the rapid burn angle and the flame development angle is marked in the figure

### 3.4 Pressure at IVC

The pressure at IVC can be approximated to be equal to the pressure at the intake manifold or as in equation (3.21). The equation depends on the rotational speed ( $N$ ) and two tuning parameters ( $C_1$  and  $C_2$ ).

$$p_{ivc} = p_{im}(\theta_{ivc}) + c_1 + c_2N \quad (3.21)$$

Equation 3.21 can be solved with a simple least square method if the pressure at IVC and the intake manifold is known.

### 3.5 Gatowski

The first pressure model that is presented is a differential-based pressure model by Gatowski which includes heat transfer in the cylinder. The model can be used to calculate the pressure in the cylinder if the heat release trace is known or the heat release trace of the pressure in the cylinder is known. Since the heat release trace is known from previous methods, the Gatowski method is stated as

$$dp = \frac{dQ_{ch} - \frac{c_v(T)+R}{R}pdV - dQ_{ht}}{\frac{c_v(T)}{R}V + \frac{V_{cr}}{RT_w} \left( u(T') - u(T) + RT' + c_v(T)T \right)} \quad (3.22)$$

where the volume and the derivative volume is calculated by

$$V(\theta) = V_d \left[ \frac{1}{r_c - 1} + \frac{1}{2} \left( \frac{l}{1} + 1 - \cos(\theta) - \sqrt{\left( \frac{l}{1} \right)^2 - \sin^2(\theta)} \right) \right] \quad (3.23)$$

$$\frac{dV}{d\theta} = \frac{1}{2} V_d \sin(\theta) \left( 1 + \frac{\cos(\theta)}{\sqrt{\left(\frac{l}{l}\right)^2 - \sin^2(\theta)}} \right) \quad (3.24)$$

The pressure derivative is calculated by

$$\frac{dp}{d\theta} = \frac{p(\theta_{i+1}) - p(\theta_{i-1})}{\theta_{i+1} - \theta_{i-1}} \quad (3.25)$$

### 3.5.1 Heat release rate

The heat release rate ( $dQ_{ch}$ ) depends on the fuel mass, the lower heat value of the fuel ( $q_{HLV}$ ), the combustion efficiency ( $\eta_f$ ) and the MFB trace as in equation (3.26).

$$\frac{dQ_{ch}}{d\theta} = m_f q_{HLV} \eta_f \frac{x_b}{d\theta} \quad (3.26)$$

The fuel mass ( $m_f$ ) is modelled as equation (3.27)

$$m_f = \frac{1 - x_r}{1 + \lambda\left(\frac{A}{F}\right)_s} \frac{p_{ivc} V_{ivc}}{RT_{ivc}} \quad (3.27)$$

where  $x_r$  is the amount of residual gases. With equation (3.26) and equation (3.27), the heat release rate can be modelled as

$$\frac{dQ_{ch}}{d\theta} = Q_{in} \frac{x_b}{d\theta} = \left( \frac{1 - x_r}{1 + \lambda\left(\frac{A}{F}\right)_s} \frac{p_{ivc} V_{ivc}}{RT_{ivc}} \eta_f q_{LHV} \right) \frac{x_b}{d\theta} \quad (3.28)$$

where ( $Q_{in}$ ) is the total chemical energy in the system, which is the amount of fuel times the lower heating value of the fuel and the combustion efficiency. Depending on the operation condition, the combustion efficiency varies and need to be taken into account. When determining the residual gases, an iteration method is used as describes in [6]. The method uses the relationship between the residual gases, the specific heat supplied the system ( $q_{in}$ ), the temperature of the residual gases ( $T_r$ ) and the temperature at the intake stroke ( $T_1$ ). Both  $T_1$  and  $q_{in}$  are functions of the residual gases, therefore an iteration is needed to solve the equations below.

$$x_r = \frac{1}{r_c} \left( \frac{p_{em}}{p_{im}} \right)^{\frac{1}{\gamma}} \left( 1 + \frac{1}{c_v T_1 r_c^{\gamma-1}} \right)^{-\frac{1}{\gamma}} \quad (3.29)$$

$$q_{in} = \frac{1 - x_r}{1 + \lambda\left(\frac{A}{F}\right)_s} q_{LHV} \quad (3.30)$$

$$T_r = \left( 1 + \frac{q_{in}}{c_v T_1 r_c^{\gamma-1}} \right) \quad (3.31)$$

$$T_1 = x_r T_r + (1 - x_r) T_{im} \quad (3.32)$$

When solving the iterations, the following approach is used.

1. Start with  $x_r=0$  as the initial value and solve equation (3.30).
2. Solve (3.31) and (3.32)
3. Calculate a neq  $x_r$  with equation (3.29).
4. Repeat the steps until  $x_r$  and  $T_r$  converges

### 3.5.2 Heat Transfer

The heat transfer is mainly caused due to convection and the rate of energy transferred ( $\dot{Q}_{ht}$ ) is modelled with Newton 's law of cooling as in Klein [19],

$$\dot{Q}_{ht} = \frac{dQ_{ht}}{d\theta} \omega_e = h_c A (T - T_w) \frac{60}{2\pi N} \quad (3.33)$$

where  $T_w$  is the cylinder wall temperature,  $N$  is the engine speed in rpm,  $h_c$  is the convection heat transfer coefficient and  $A$  is the surface area in the cylinder and calculated by

$$A = \pi \frac{B^2}{2} + \pi B(l + a - s) + B\pi \frac{L}{r_c - 1} \quad (3.34)$$

The convection heat transfer coefficient is influenced by many parameters. One way of modelling the convection heat transfer is proposed by Woschni as in Klein [19]

$$h_c = \frac{0.013 B^{-0.2} p^{0.8} \left( C_1 u_p + \frac{C_2 (p - p_0) T_r V}{p_r V_r} \right)^{0.8}}{T^{0.55}} \quad (3.35)$$

In this equation  $p$  is the pressure,  $p_0$  is the motored pressure,  $T$  is temperature,  $u_p$  is the mean piston speed,  $V$  is the volume,  $C_1$  and  $C_2$  are two design parameters. The parameters with index  $r$ , are constant values at a reference point. Typical values for the design parameters are suggested in Eriksson and Nielsen [6] as in table 3.1.

**Table 3.1:** Suggested values on  $C_1$  and  $C_2$

	Gas exchange	Compression	Combustion and expansion m/s
$C_1$	6.18	2.28	2.28
$C_2$	0	0	0.00325

### 3.5.3 Specific heat ratio

The model for the gas properties is the most important parameter when modelling the pressure with Gatowski [7]. There are many different approaches when modelling the specific heat ratio. Two different methods are presented, a linear function by Gatowski et al. [10] and a modification of the linear model presented in Eriksson and Sivertsson [7]. The linear model is stated as

$$\gamma_{lin}(T) = \gamma_{300} + b(T - 300) \quad (3.36)$$

where  $b$  and  $\gamma_{300}$  are adjusted by the temperature and the air-fuel ratio ( $\lambda$ ).

The modified model for the specific heat ratio is presented below. Note that both models are using the mean temperature that is presented in equation (3.6). This model is accurate for lean conditions, i.e.  $\lambda > 1$ , where the internal energy and the specific heat is a function of the temperature and the air/fuel ratio as equation (3.37) and equation (3.38).

$$u_s(\lambda, \tilde{T}) = l_1 \lambda \tilde{T} + l_2 \lambda \tilde{T}^2 + l_3 \lambda^2 \tilde{T}^2 + c_1 \tilde{T} + c_2 \tilde{T}^2 + c_3 \tilde{T}^3 + c_4 \tilde{T}^4 + c_5 \tilde{T}^5 \quad (3.37)$$

$$c_v(\lambda, \tilde{T}) = \frac{l_1 \lambda + 2l_2 \lambda \tilde{T} + 2l_3 \lambda^2 \tilde{T} + c_1 + 2c_2 \tilde{T} + 3c_3 \tilde{T}^2 + 4c_4 \tilde{T}^3 + 5c_5 \tilde{T}^4}{1000} \quad (3.38)$$

where

$$\tilde{T} = \frac{T - 300}{1000} \quad (3.39)$$

The absolute internal energy ( $u_{300}$ ) is a second order polynomial in  $\lambda$ ,

$$u_{300}(\lambda) = u_0 + u_1 \lambda + u_2 \lambda^2 \quad (3.40)$$

The final expression for the internal energy is achieved by combining equation (3.37) and equation (3.40),

$$u(\lambda, T) = u_{300}(\lambda) + u_s(\lambda, \tilde{T}(T)) \quad (3.41)$$

In table 3.2 the parameters for the modified model is presented.

**Table 3.2:** Parameters for the modified model

Parameter	Value
$c_1$	$+8.26159 \cdot 10^5$
$c_2$	$+1.65422 \cdot 10^5$
$c_3$	$+1.02150 \cdot 10^5$
$c_4$	$-0.85770 \cdot 10^5$
$c_5$	$+0.21236 \cdot 10^5$
$l_1$	$-0.39486 \cdot 10^5$
$l_2$	$-0.90978 \cdot 10^5$
$l_3$	$+0.26322 \cdot 10^5$
$u_0$	$-6.20236 \cdot 10^6$
$u_1$	$+4.13857 \cdot 10^6$
$u_2$	$-0.91531 \cdot 10^6$

To get a better understanding of how these two models differs from each other one can model the specific heat ratio as

$$\gamma = \frac{c_v + R}{c_v} \quad (3.42)$$

where  $R$  is the gas constant of air. In figure 3.3 an example of the shape for the specific heat ratios for the two methods are presented.

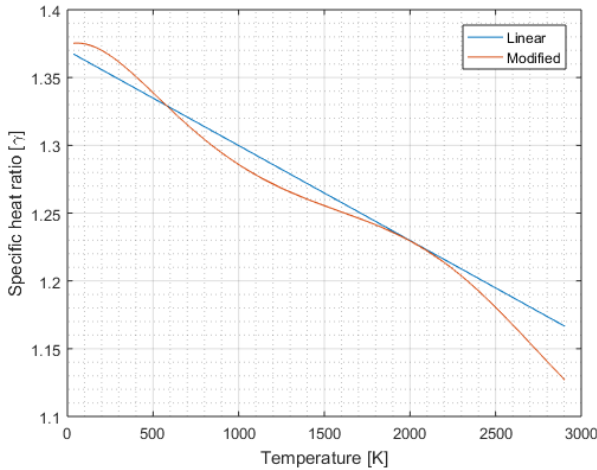


Figure 3.3: The two different methods of modelling the specific heat ratio

### 3.5.4 Crevice model

The crevice model make allowances for minor losses in the cylinder where some of the fuel flows into the crevice and stays there during the combustion. When modelling the losses due to the crevice, the temperature is approximated to be close to the cylinder wall temperature ( $T_w$ ). The crevice volume ( $V_{cr}$ ) is assumed to be 1.5% of the total clearance volume ( $V_c$ ). In equation (3.22) the crevice model parameters are marked with a prime.

## 3.6 Analytic cylinder pressure Model

The second pressure model is an analytic cylinder pressure model. The in-cylinder pressure trace is based on the ideal Otto cycle. The model is dividing the engine cycle into two different parts in Eriksson and Andersson [5].

### 3.6.1 Compression Asymptote

The compression process can be modelled as a polytropic process. To get the modelled pressure and temperature in the cylinder, the polytropic exponent ( $\gamma_c$ ) and a reference point (IVC) is needed [5]. Equation (3.43) and (3.44) describes the pressure and the temperature during compression until the combustion starts.

$$p_c(\theta) = p_{ivc} \left( \frac{V_{ivc}}{V(\theta)} \right)^{\gamma_c} \quad (3.43)$$

$$T_c(\theta) = T_{ivc} \left( \frac{V_{ivc}}{V(\theta)} \right)^{\gamma_c - 1} \quad (3.44)$$

The temperature at IVC is a very complex variable to determine since it depends on residual gases and heat transfer in the cylinder. Therefore, a simplified model is used. The model assume that the specific heat ( $c_p$ ) for the air and fuel mixture is the same as for the residual gases. The temperature at IVC is calculated with equation (3.45) as

$$T_{ivc} = T_{\alpha f}(1 - x_r) + x_r T_r \quad (3.45)$$

where  $T_{\alpha f}$  is simplified to be  $T_{im}$  when the heat transfer is neglected, see Eriksson and Nielsen [6]. When determining the residual gases ( $x_r$ ) the same iteration method as in section 3.5.1 is used.

### 3.6.2 Expansion Asymptote

The expansion process can also be modelled by a polytropic process with a polytropic exponent ( $\gamma_e$ ) as

$$p_e(\theta) = p_3 \left( \frac{V_3}{V(\theta)} \right)^{\gamma_e} \quad (3.46)$$

$$T_e(\theta) = T_3 \left( \frac{V_3}{V(\theta)} \right)^{\gamma_e - 1} \quad (3.47)$$

where the variables  $p_3$ ,  $T_3$  and  $V_3$  refers to the third state in the ideal Otto cycle [6]. The parameters at the third state can be determined by going from second state with a temperature increase ( $\Delta T_{comb}$ ) as

$$\Delta T_{comb} = \frac{(1 - x_r)q_{LHV}\eta_f(\lambda)}{(\lambda(A/F)_s + 1)c_v} \quad (3.48)$$

where the temperature during at the third state is modelled as

$$T_3 = T_2 + \Delta T_{comb} \quad (3.49)$$

The equation for the fuel conversion efficiency ( $\eta_f$ ) is modelled as in Heywood [12] with the following equation

$$\eta_f(\lambda) = 0.95 \min(1; 1.2\lambda - 0.2) \quad (3.50)$$

The ideal gas law gives the pressure at the third state as

$$p_3 = p_2 \frac{T_3}{T_2} \quad (3.51)$$

where the temperature and pressure at the second state is determined with equations (3.43) and (3.44) at SOC.

### 3.6.3 Combustion

When the two asymptotes are known the combustion process can be interpolated using the Vibe function as equation (3.17). The pressure in the cylinder during the combustion is modelled as

$$p_{cyl}(\theta) = (1 - x_b(\theta))p_c(\theta) + x_b(\theta)p_e(\theta) \quad (3.52)$$

### 3.6.4 Gas exchange

To model the complete pressure curve the effects of the gas exchange needs to be modelled. This happens when the exhaust valve opens and the cylinder pressure start to decline to the exhaust pressure. The following interpolation between the two phases are used

$$x_i(\theta, \theta_{evo}, \theta_{exh}) = \frac{1}{2} \left( 1 - \cos \left( \pi \frac{\theta - \theta_{evo}}{\theta_{exh} - \theta_{evo}} \right) \right) \quad (3.53)$$

where the cylinder pressure is modelled as

$$p_{cyl} = (1 - x_i(\theta, \theta_{evo}, \theta_{exh}))p_e(\theta) + x_i(\theta, \theta_{evo}, \theta_{exh})p_{em} \quad (3.54)$$

### 3.6.5 Complete pressure model

The complete pressure curve can now be modelled with equation (3.55).

$$p_{cyl}(\theta) = \begin{cases} p_{im} & \text{if } \theta_{evc} \leq \theta < \theta_{int} \\ p_c(\theta) & \text{if } \theta_{ivc} \leq \theta < \theta_{soc} \\ (1 - x_b(\theta))p_c(\theta) + x_b(\theta)p_e(\theta) & \text{if } \theta_{soc} \leq \theta < \theta_{evo} \\ (1 - x_i(\theta, \theta_{evo}, \theta_{exh}))p_e(\theta) + x_i(\theta, \theta_{evo}, \theta_{exh})p_{em} & \text{if } \theta_{evo} \leq \theta < \theta_{exh} \\ p_{em} & \text{if } \theta_{exh} \leq \theta < \theta_{ivo} \end{cases} \quad (3.55)$$

### 3.7 Summary of the in-cylinder models

Cylinder volume (3.23), (3.24)

$$V(\theta) = V_d \left[ \frac{1}{r_c - 1} + \frac{1}{2} \left( \frac{l}{1} + 1 - \cos(\theta) - \sqrt{\left(\frac{l}{1}\right)^2 - \sin^2(\theta)} \right) \right]$$

$$\frac{dV}{d\theta} = \frac{1}{2} V_d \sin(\theta) \left( 1 + \frac{\cos(\theta)}{\sqrt{\left(\frac{l}{1}\right)^2 - \sin^2(\theta)}} \right)$$

Temperature model (3.6), (3.11).

$$T(\theta) = \frac{T_{ivc}}{p_{ivc} V_{ivc}} p(\theta) V(\theta)$$

$$T_u(\theta) = \begin{cases} \frac{T_{ivc}}{p_{ivc} V_{ivc}} p(\theta) V(\theta) & \text{if } \theta \leq \theta_{soc} \\ T_{u,soc} \left( \frac{p(\theta)}{p_{soc}} \right)^{\frac{\gamma-1}{\gamma}} & \text{if } \theta > \theta_{soc} \end{cases}$$

Vibe model (3.17), (3.18), (3.19).

$$x_b(\theta) = \begin{cases} 0 & \theta < \theta_{ign} \\ 1 - e^{-a \left( \frac{\theta - \theta_{ign}}{\Delta\theta} \right)^{m+1}} & \theta \geq \theta_{ign} \end{cases}$$

$$m = \frac{\ln \left( \frac{\ln(1-0.1)}{\ln(1-0.85)} \right)}{\ln(\Delta\theta_d) - \ln(\Delta\theta_d) + \Delta\theta_b} - 1$$

$$a = -\ln(1 - 0.1) \left( \frac{\theta}{\theta_d} \right)^{m+1}$$

Gatowski pressure model (3.22).

$$dp = \frac{dQ_{ch} - \frac{c_v(T)+R}{R} p dV - dQ_{ht}}{\frac{c_v(T)}{R} V + \frac{V_{cr}}{RT_w} \left( u(T') - u(T) + RT' + c_v(T)T \right)}$$

Analytic pressure model (3.55)

$$p_{cyl}(\theta) = \begin{cases} p_{im} & \text{if } \theta_{evc} \leq \theta < \theta_{int} \\ p_c(\theta) & \text{if } \theta_{ivc} \leq \theta < \theta_{soc} \\ (1 - x_b(\theta))p_c(\theta) + x_b(\theta)p_e(\theta) & \text{if } \theta_{soc} \leq \theta < \theta_{evo} \\ (1 - x_i(\theta, \theta_{evo}, \theta_{exh}))p_e(\theta) + x_i(\theta, \theta_{evo}, \theta_{exh})p_{em} & \text{if } \theta_{evo} \leq \theta < \theta_{exh} \\ p_{em} & \text{if } \theta_{exh} \leq \theta < \theta_{ivo} \end{cases}$$

### 3.8 Polynomial models for the combustion parameters

To be able to make the model independent and to extend the model from the operation points in the experimental data, it is necessary to make polynomial models for the combustion parameters. The main idea with this modelling strategy is that input parameters are sent to the polynomial models. The polynomial models then interpolates and sends the parameters needed to the pressure model. In figure 3.4 an overview of the independent model can be seen.

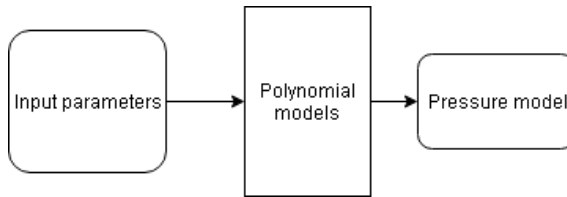


**Figure 3.4:** Shows the working principal for the polynomial models.

The input parameters that are necessary can be seen in table 3.3. Note that the pressure model has more input parameters like temperatures etc. These parameters go straight to the pressure model since they do not have a direct impact on the parameters calculated in the polynomial models.

**Table 3.3:** Shows the input parameters for the polynomial models.

Input parameter	Description
$N$	Engine speed [rpm]
$P_{im}$	Intake manifold pressure [Pa]
$VVT$	Variable valve timing [Deg]
$\theta_{ign}$	Ignition angle [Deg]
$\lambda$	Air-fuel ratio [-]

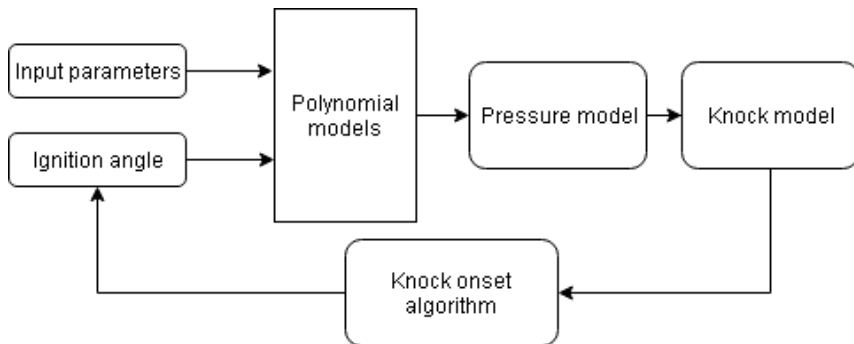
The parameters that are needed from the polynomial models depends on which pressure model that is used. Common parameters for both models are the ignition parameters such as the rapid burn angle, flame development angle and the ignition efficiency, see table 3.4. Operation points with engine speed between 1000-4500 rpm at different engine torques are used to create the polynomial models. For each operation point, 10 cycles out of 50 cycles were used to create the polynomial models. The goal is to create polynomials that describes the parameters in table 3.4 based on the input parameters seen in table 3.3.

**Table 3.4:** Parameters for the polynomial models

Parameter	Description
$\Delta\theta_d$	Flame development angle [deg]
$\Delta\theta_b$	Rapid burn angle [deg]
$\eta_{ign}$	Ignition efficiency [-]
$\gamma_c$	Polytropic coef. for compression [-]
$\gamma_e$	Polytropic coef. for expansion [-]

### 3.9 Knock prediction model

To be able to make a model that can predict knock onset, the independent pressure model with polynomial models has to be connected to the knock model. The idea with this strategy is that the input parameters and the initial guess for the ignition angle is sent to the polynomial models. The output parameters from the polynomial models are then sent to the pressure model which simulates a pressure trace. The trace is then sent to the knock model which calculates the knock integral at MFB95. The value of the knock integral will tell if the engine will knock or not in that specific operation point. If the engine is about to knock, the igniting angle will be retarded. If the engine will not knock, the ignition angle will be advanced. The model will be iterated until the knock model shows knock onset. In figure 3.5 an overview of the knock prediction model can be seen.

**Figure 3.5:** An overview of the knock prediction model

#### 3.9.1 Knock onset algorithm

As mentioned in section 3.9, the knock prediction model works by iterating for different ignition angle until knock onset is detected. This working principal for the iterations can be seen in figure 3.6.

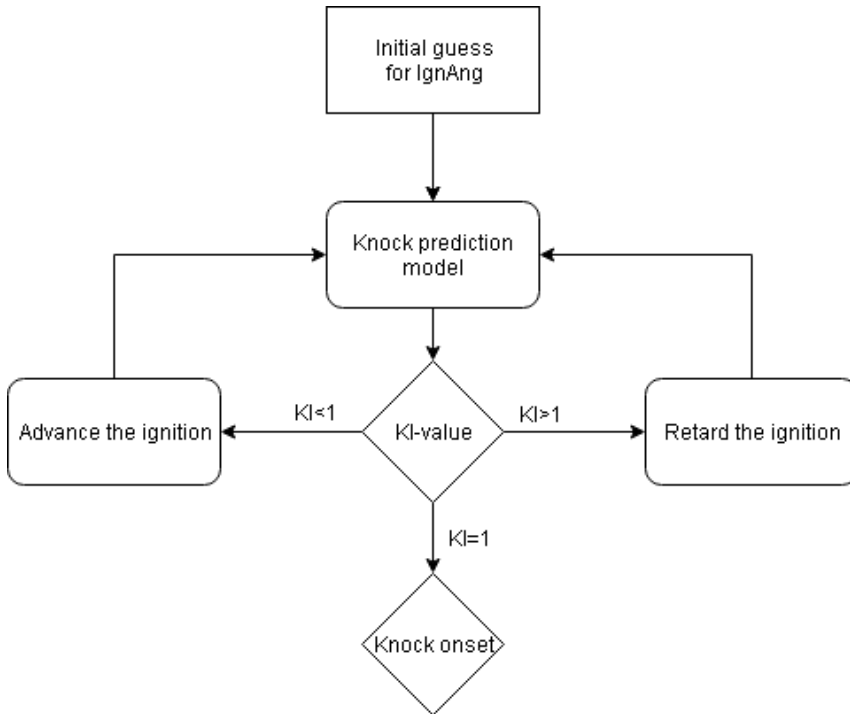


**Figure 3.6:** Describes the working principal for the iterations of the ignition angle. Based on the value of the knock integral, the ignition angle will be advanced or retarded until knock onset is detected.

To make the model as fast and accurate as possible, it is necessary to have an algorithm which determines the ignition angle for the next iteration. The algorithm may use data saved from previous iterations.

The algorithm that were chosen for the iterations is using linear approximations. Based on the previous 2 values of the ignition angle and knock index, the next ignition angle will be calculated using the gradient of the two points in a diagram of the knock integral and ignition angle. The algorithm will work in 3 steps which will be described below.

1. The first step is to run the model with an initial value for the ignition angle. The calculated value of the knock integral is then saved as iteration number one.
2. The second step is to run the model with a different ignition angle. Based on the value of the knock integral from iteration number one, the ignition angle will be advanced or retarded with a fixed amount. If the integral shows below 1, the ignition angle will be advanced a fixed amount. If the integral shows above 1, the ignition angle will be retarded a fixed amount.
3. In the third step the gradient between the last two iterations is calculated

using equation (3.56). The gradient is then used in equation (3.57) to calculate the next Ignition angle. This equation also uses the previous ignition angle as well as the difference between 1 and the knock integral in previous iteration. This step will be looped until the the knock integral is equal or close to 1 i.e. knock onset.

$$k(i) = \frac{\theta_{ign}(i) - \theta_{ign}(i-1)}{KI(i) - KI(i-1)} \quad (3.56)$$

$$\theta_{ign}(i) = \theta_{ign}(i-1) + (1 - KI(i-1)) \cdot k(i-1) \quad (3.57)$$



# 4

---

## Data processing

This chapter gives an overview of the methods for the data processing that are necessary before implementing it into the models. First, the engine specification and the data structure are explained and later some methods to process the data is presented.

### 4.1 Data description

The data used for modeling is gathered either from Volvo Cars or Vehicle Systems engine lab at Linköping University.

#### 4.1.1 Engine data

The engine that is used is a 2 liter, 4-cylinder SI-engine. The engine specification can be seen in table 4.1.

*Table 4.1: Engine specification*

Parameter	Description	Value
B	Bore	82 mm
l	Connecting rod length	144.2 mm
a	Crank radius	46.6 mm
L	Piston stroke	93.2 mm
$r_c$	Compression ratio	10.8:1

### 4.1.2 Measured data

The measured data used in this project has its source in different test rigs but with the same sort of engine. Most of the data is from a test rig at Volvo Cars and some of the data is from the test rig at Linköping University. The data is split into two sections. The data from Volvo Cars is used as building and training data for the model. The data from Linköping University is used as validation data.

The data obtained was at engine speeds between 1000-5000 rpm at different torques, ignition angles, cam phasing etc. Each operation point have 50 measured cycles on all four cylinders, so in total 200 pressure traces per operation point. During some operation points, the ignition timing varies due to the knock controller that retards the ignition timing if knock occur. Therefore, no data of the exact ignition timing were given for these cycles. To get an understanding of where the combustion should start one could use the heat release analysis and the MFB to approximate where the combustion starts. The sample frequency of the pressure signal varies during the cycle. Between the interval  $-359 < \theta \leq 0$  and  $40 \leq \theta < 360$  there are one measurement per crank angle. Between  $0 < \theta < 40$  there are 10 measurements per crank angle. This allows for a better accuracy when detecting knock during the combustion phase.

## 4.2 Pressure pegging

In the modelling process, one of the most important parameter is the cylinder pressure. Therefore, it is necessary to validate the measured pressure to make it more trustworthy. This is done by using the pressure sensor in the intake manifold. The pressure sensor in the cylinder, compared to the intake manifold sensor, is working over a wider pressure range which will make the intake manifold sensor more accurate at low pressures. In theory, the pressure in the intake manifold and the cylinder will be the same right before IVC. A plot over the pressure in the intake manifold and the cylinder pressure can be seen in figure 4.1.

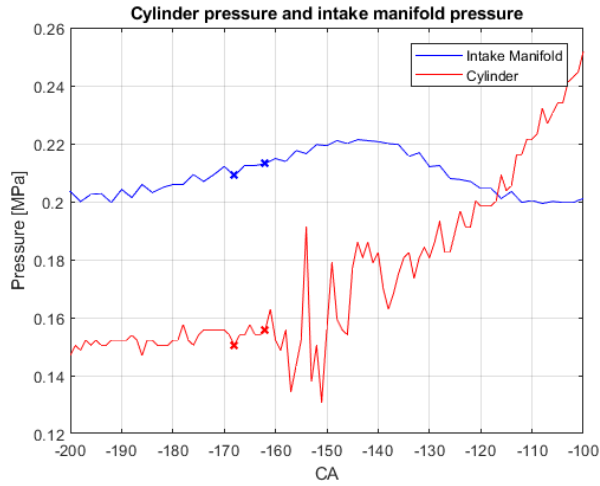


**Figure 4.1:** Shows the pressure in the intake manifold and in the cylinder. The crosses are placed at  $CA=-167^\circ$  and  $CA=-162^\circ$ . The IVC is placed around  $CA=-160^\circ$ .

As seen in figure 4.1, the pressure differs a bit even though the pressures are in fact very close to each other. A mean value between the crosses is therefore calculated. The difference between those two mean values is then used as an offset for the whole cylinder pressure curve. The modified pressure curve can be seen in figure 4.2.

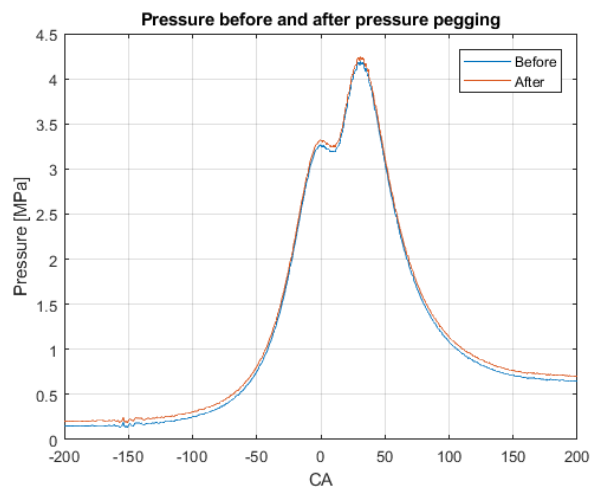


**Figure 4.2:** Shows the Pressure curve before and after the pressure pegging.

### 4.3 Filter the measurement signal

The pressure sensors inside the cylinder is very sensitive and may in some cases get affected by noise due to vibrations from the crank shaft. To eliminate the risk of great errors in further calculations, it is necessary to get rid of the noise. This is done by implementing a low pass filter. The filter is designed by doing a rough Fast Fourier transform (FFT) analysis. A cut off frequency is chosen based on a spectrum and tuned until most of the noise in the pressure curve was eliminated. Figure 4.3 shows a pressure curve before and after the implementation of the low pass filter.

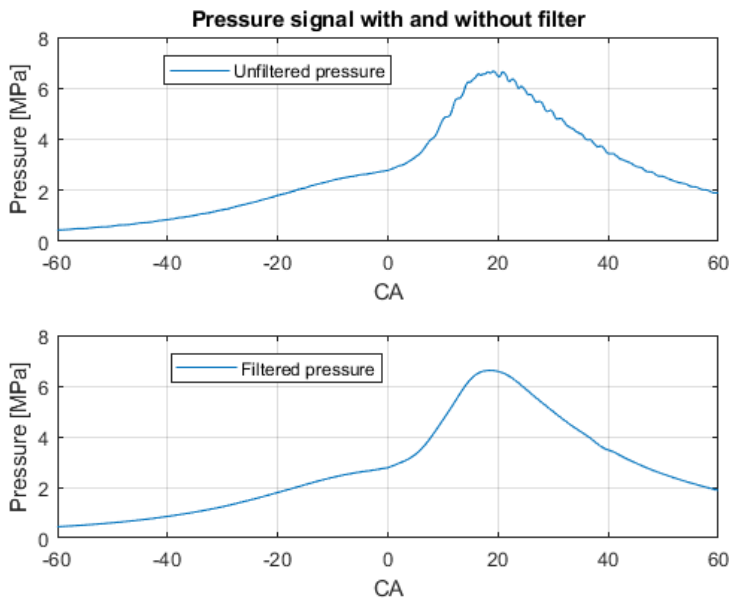


*Figure 4.3: Shows the pressure curve before and after the low pass filter were implemented.*

### 4.4 Knock onset

Knock onset refers to what crank angle knock occur. To identify knock onset on a measured pressure curve it is important to understand that there is a lot of noise that not should be mixed together with the pressure oscillations due to knock. One effective way to identify knock is to implement a high pass filter that only show the pressure oscillations due to knock. This technique has been used in Elmqvist et al. [3] with great results. To design the high pass filter, a FFT analysis is done on the pressure curve. Figure 4.4 shows a spectrum of a pressure curve where knock occur.

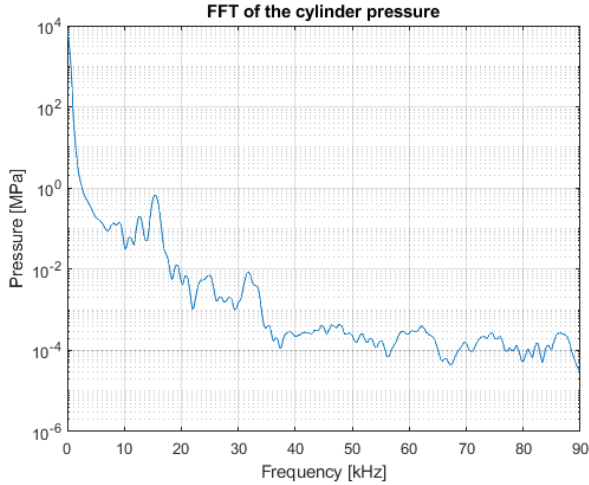


**Figure 4.4:** Shows a spectrum over a pressure curve with knock. The spectrum shows a lot of energy between 10 and 40 kHz.

As seen in figure 4.4, there are two large peaks around 15 and 32 kHz. The cut off frequency is therefore chosen to be 10 kHz. Figure 4.5 shows an example of measured pressure trace before and after it is filtered with the high pass filter.

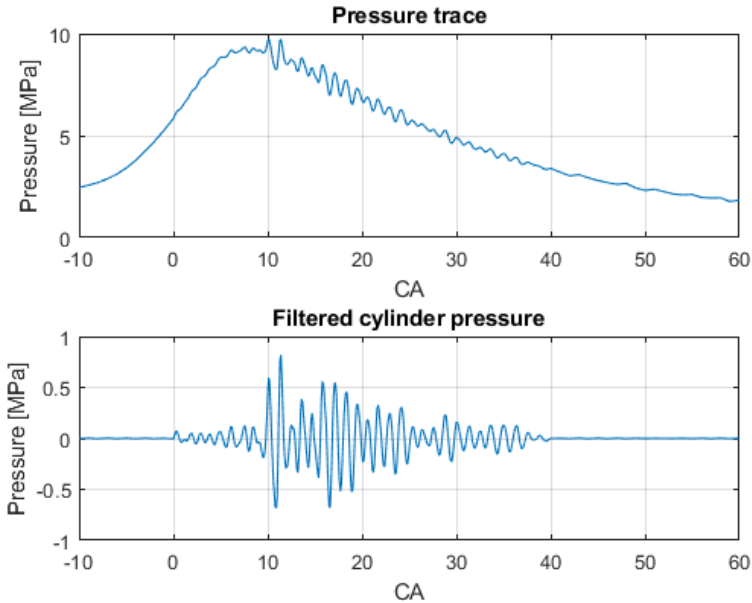


**Figure 4.5:** The upper plot shows a pressure trace and the lower plot shows the pressure after the high pass filter is applied.

The idea is to use the filtered pressure trace and use a Matlab script that determines at what crank angle the pressure oscillations rise above a certain value, which corresponds to knock onset. This value is later used to validate the knock model and the goal is to get the modeled knock onset close to the measured knock onset.

#### 4.4.1 Tuning the coefficients in the knock model

As mention in section 3.1, the coefficients in the knock model needs to be tuned to fit the measured data. By combining equation (3.1) and equation (3.2) with the knowledge that the knock integral should be equal to one when knock occur, the following equation can be stated

$$KI = \int_{\theta_{ivc}}^{\theta_{KO}} \frac{1}{X_1 \cdot p^{-X_2} \cdot e^{\frac{X_3}{T_u}}} d\theta = 1 \quad (4.1)$$

This nonlinear equation is solved with the Matlab function *lsqnonlin* which is a nonlinear least-squares solver. The steps that made to fit the coefficient are:

- Find several cycles with knock at different operation conditions. If the knock is light (low pressure oscillations) the model sensitivity will be higher and therefore more accurate when comparing measured knock onset and model knock onset.
- Run each cycle in the knock model and use the measured pressure and the modelled unburned temperature to solve equation (4.1). The starting values for the coefficients are stated earlier in equation (3.3).
- Use *lsqnonlin* and solve the following function

$$MinFunction = 1 - KI$$

where the coefficient  $X_1$ ,  $X_2$  and  $X_3$  are optimized to minimize the function.

- Run the knock model with the new values. If the knock integral is close to one at every cycle the optimized values are good. Otherwise, one could change the upper/lower boundaries in *lsqnonlin* or modify the coefficients. In other researches, the coefficients  $X_2$  were engine speed dependent which allows for a better accuracy between different operation conditions.

# 5

---

## Result and discussion

This chapter will cover the result of each model presented in chapter 3. The result is presented in the same order as the modelling was done, which will facilitate the understanding of the modelling strategy.

### 5.1 Knock onset

As from section 4.4, knock onset was detected with a high pass filter. The limits for the pressure oscillations that corresponds to knock onset can be seen in table 5.1, where knock onset is set to be the first peak that overcomes the limit value.

*Table 5.1: The knock onset oscillation limit for different engine speeds.*

Engine speed [rpm]	Knock onset limit [MPa]
$N \leq 1500$	0.085
$1500 < N < 2500$	0.15
$N \geq 2500$	0.32

The result for two different operation cycles can be seen in figure 5.1 and figure 5.2. The top plot shows the pressure curve and the bottom shows the high pass filtered pressure. In each plot, a cross can be seen which marks the crank angle where knock onset is detected.

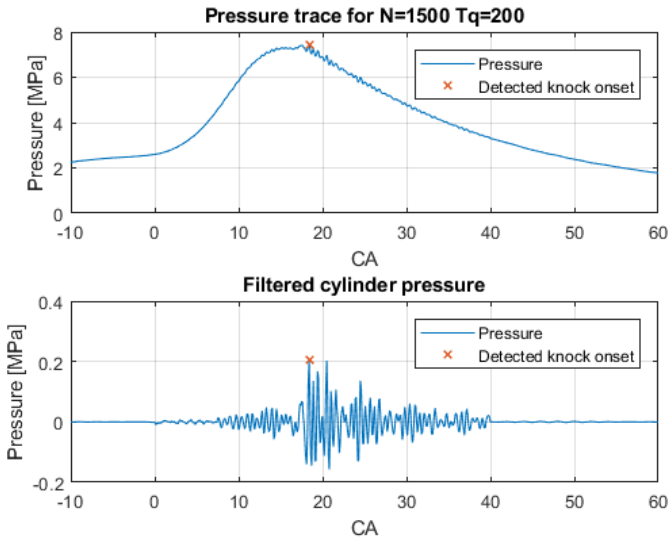


**Figure 5.1:** The limits that are used to determine knock onset from the filtered pressure curve at Engine speed = 1500 rpm and Torque = 200 Nm

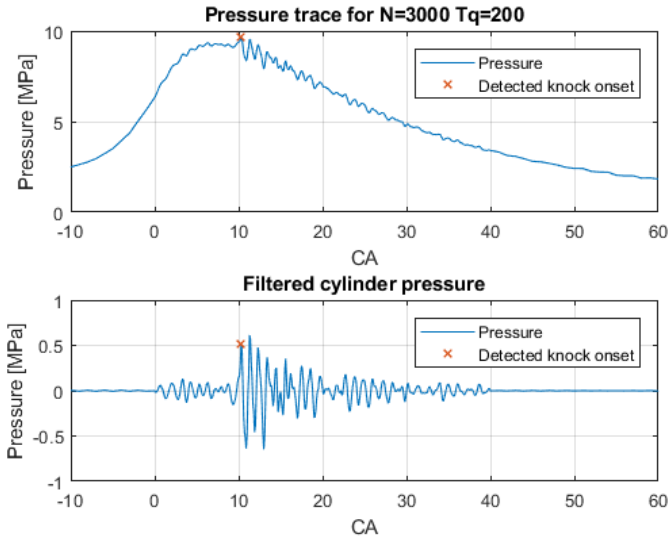


**Figure 5.2:** The limits that are used to determine knock onset from the filtered pressure curve at Engine speed = 3000 rpm and Torque = 200 Nm

This method of detecting knock was relative good at engine speed up to 3000 rpm. At higher engine speed, the noise was larger due to more vibrations on the

engine block. These vibrations causes more noise which lead to a big uncertainty when setting the knock onset limit due to inconsequent pressure oscillations in the filtered pressure curve.

### 5.1.1 Tuning the knock model

The tuning was done with engine speeds between 1000-3000 rpm and torque range of 150-200 Nm. In total, 300 cycles where found where the knock controller was active. Only 49 of these cycles had knock detected through the high pass filter. The parameters that were optimized can be seen in table 5.2.

**Table 5.2:** Knock model coefficients optimized with 49 cycles with engine speed between 1000-3000 rpm and torque between 150-200 Nm

Parameter	Value
$X_1$	14.2126
$X_2$	1.7278
$X_3$	3006.9

Figure 5.3 shows the accuracy of the knock model with the model coefficient mention in table 5.3. The optimization were done with 49 knocking cycles at different operation conditions. As seen, most cycles with knock were found at 2000 rpm and the non linear least square method will therefore prioritize to minimize these cycles. To solve this problem, different coefficients for different engine speeds were implemented.

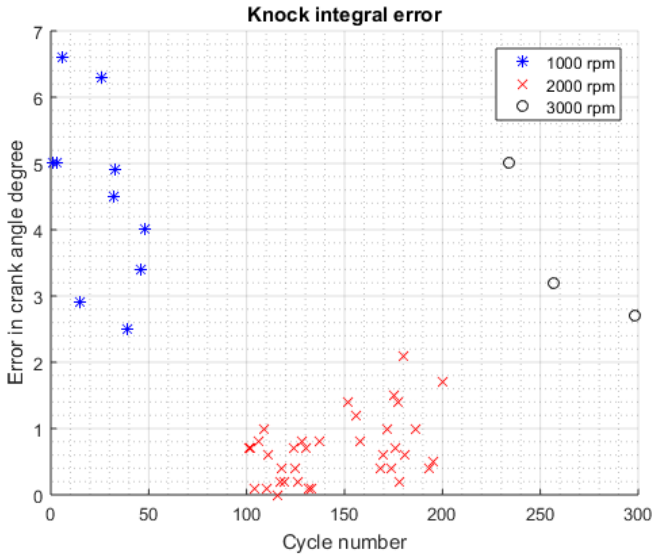
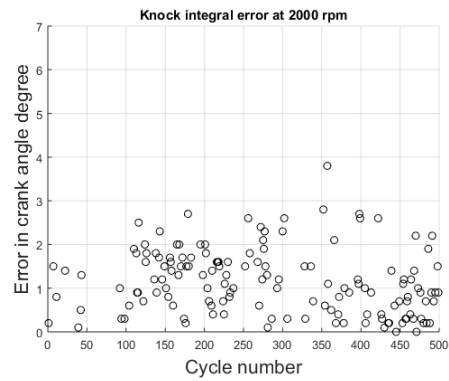
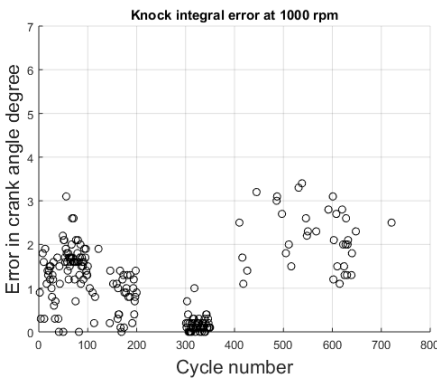


**Figure 5.3:** Show the error between measured knock onset and the model knock onset.

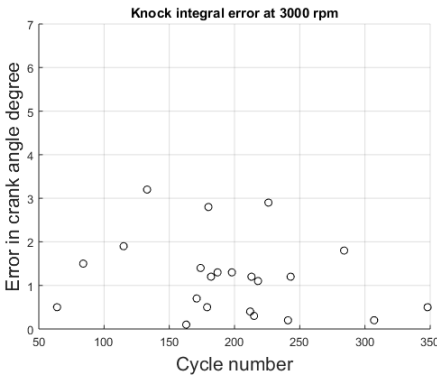
The coefficients will change value dependent of the engine speed with the goal to minimize the error as much as possible. The new coefficients were optimized with several cycles with knock at 1000, 2000 and 3000 rpm. The new coefficients can be seen in table 5.3 and the total error is presented in figure 5.4.

**Table 5.3:** Knock model coefficients for different engine speeds.

Engine speed	$X_1$	$X_2$	$X_3$
1000	18.2317	1.3469	1000
2000	22.6283	1.5546	2079.9
3000	18.8064	1.5679	2545.6



(a) Engine speed  $N = 1500$  RPM, torque  $Tq = 110$  Nm (b) Engine speed  $N = 2000$  RPM, torque  $Tq = 220$  Nm



(c) Engine speed  $N = 3000$  RPM, torque  $Tq = 195$  Nm

**Figure 5.4:** The error in the knock integral when the coefficient in the knock model is dependent on the engine speed

As seen in figure 5.4, when the coefficients changes to be dependent on the

engine speed, the total error in the knock model can be reduced. On all three engine speeds, the maximum error was smaller than 4 crank angle degrees which is seen as a good result.

## 5.2 Unburned Temperatures

The unburned temperature is modeled using equation (3.11), which is based on the ideal gas law. This temperature is not measured and is therefore hard to validate. In theory, with increasing engine speed the unburned temperature should increase because the temperature in the cylinder will be higher. As seen in figure 5.5, the unburned temperature will increase as the engine speed increases.

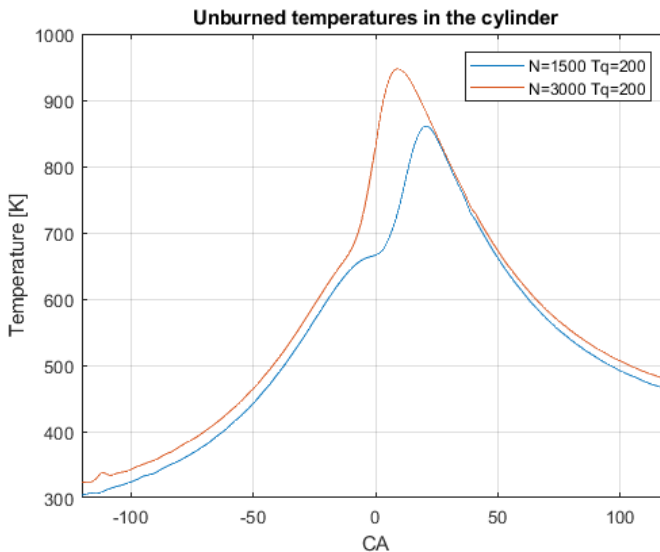
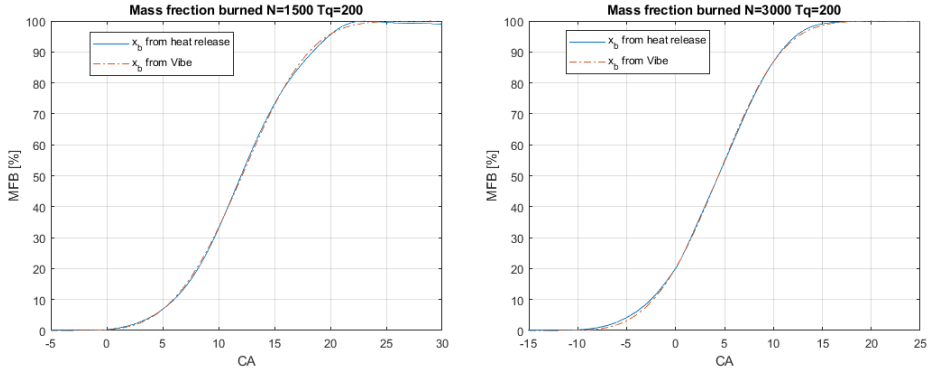


**Figure 5.5:** Shows the modeled unburned temperature in the cylinder for two different cycles. The cycle with  $N=1500$  rpm has its SOC around  $CA=-2^\circ$  and the one with  $N=3000$  has its SOC around  $CA=-15^\circ$

## 5.3 Heat release analysis and mass fraction burned

As from section 3.3, the heat release is calculated based on the thermodynamic laws. The heat release was then normalized between zero and one to show the mass fraction burned trace. Based on the MFB trace, the Vibe parameters were determined using least mean square. Figure 5.6a and 5.6b shows the calculated MFB and the MFB from vibe for two different operation conditions.



(a) MFB for a cycle with  $N=1500$  and (b) MFB for a cycle with  $N=3000$  and  $Tq=200$ .

**Figure 5.6:** MFB from heat release and the vibe function.

In both figures the Vibe function is able to match the heat release curve and can therefore be used when simulating the combustion process with good accuracy.

## 5.4 Pressure at IVC

As mentioned before, the pressure at IVC can either be expressed as the pressure at the intake manifold or as equation in (3.21). After some simulations it was found that the later method was needed to get an accurate pressure curve. The following expression was used for the pressure at intake valve closing

$$p_{ivc} = p_{im}(\theta_{ivc}) + c_1 + c_2 N$$

The coefficient  $c_1$  and  $c_2$  were solved with a least square method in Matlab and the values can be seen in table 5.4.

**Table 5.4:** The coefficient used in the model

Parameter	Value
$c_1$	1.1583e4
$c_2$	-1.2854

To validate the model for the pressure at IVC, the same operation point as for the measured data were tested in the model. The comparison of the measured and modeled pressure can be seen in figure 5.7 where the model pressure is in good agreement with the measured pressure.

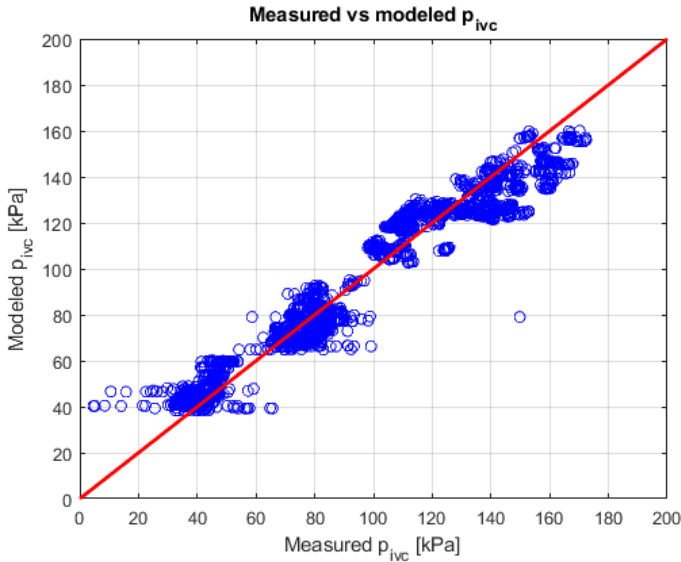


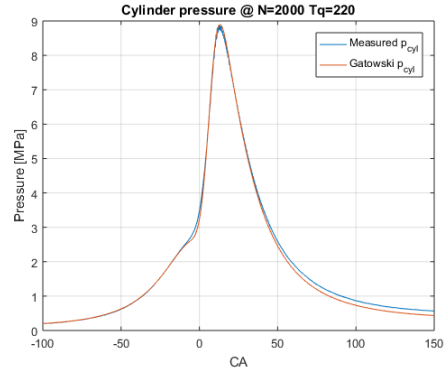
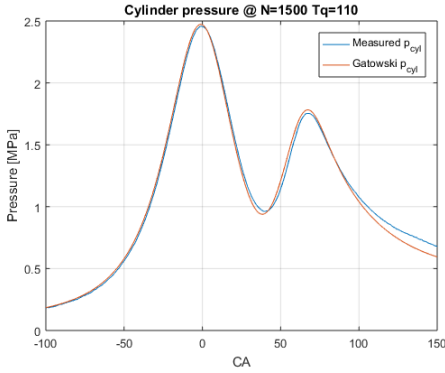
**Figure 5.7:** Shows the modeled vs the measured pressure at intake manifold. The model was tested on 2400 operation points. The red line describes the mid line for which the model pressure is the same as the measured pressure. The blue circles shows pressure at IVC at different operations points.

## 5.5 Pressure model

The modeled pressure is compared to the measured pressure for different operation points. To get a good match between the pressures, the shape of the MFB will change which also is presented. The pressure models are validated at 1500, 2000, 3000 and 4000 rpm. Engine parameters such as IVC, lambda, inlet pressure etc. were set to the correct values depending on the operation cycle and used as input parameters in the models.

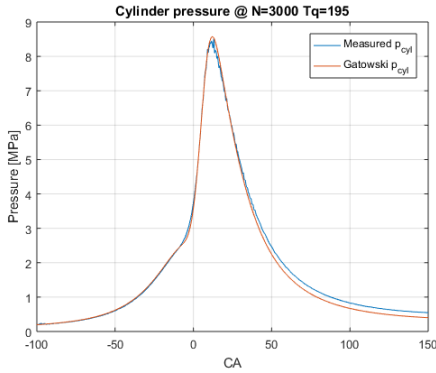
### 5.5.1 Gatowski model

As seen in figure 5.8, the model was able to simulate the cylinder pressure with good accuracy for different operation points. The most important factor when validating the pressure is the peak pressure accuracy since it has a major effect on knock. For all operation points the peak pressure is in good agreement with the measured pressure. However, during the exhaust phase the model accuracy decreases. The reason for that is probably because some physical behavior is missing in the model. In figure 5.9, the change in the MFB for the different operation cycles can be seen. No major change is seen which indicates that the Vibe function is correct and accurate.

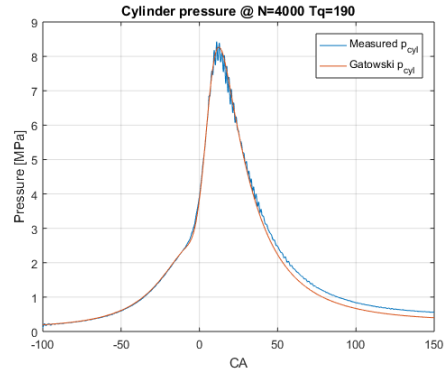


(a) Engine speed  $N = 1500$  RPM, torque  $Tq = 110$  Nm

(b) Engine speed  $N = 2000$  RPM, torque  $Tq = 220$  Nm

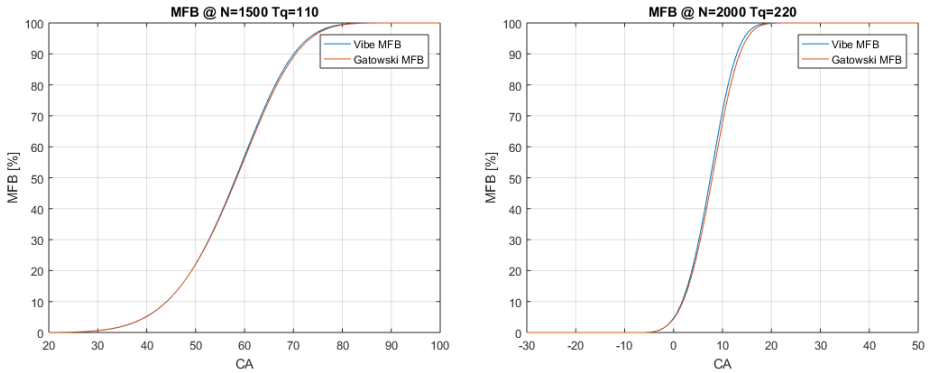


(c) Engine speed  $N = 3000$  RPM, torque  $Tq = 195$  Nm

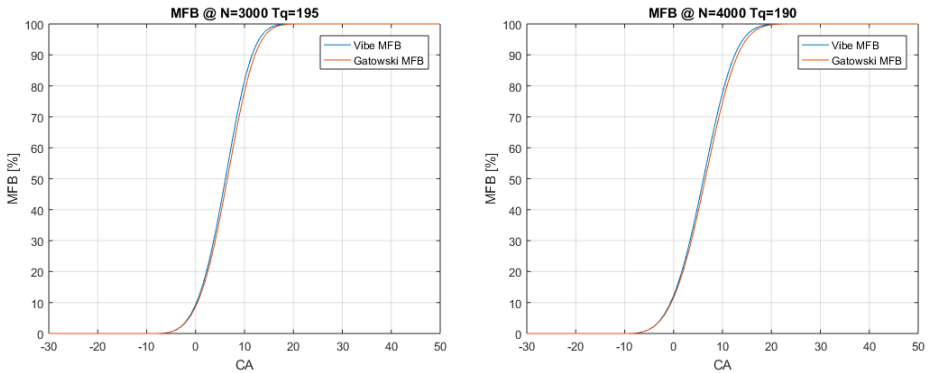


(d) Engine speed  $N = 4000$  RPM, torque  $Tq = 190$  Nm

**Figure 5.8:** Cylinder pressure for different operation cycles



(a) Engine speed  $N = 1500$  RPM, torque  $Tq = 110$  Nm (b) Engine speed  $N = 2000$  RPM, torque  $Tq = 220$  Nm

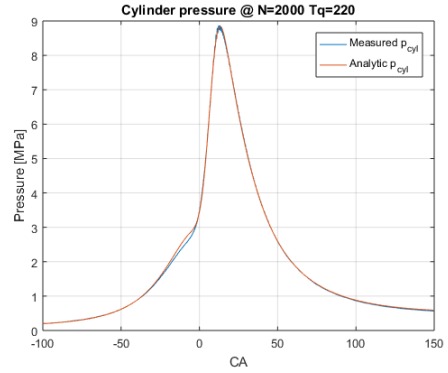
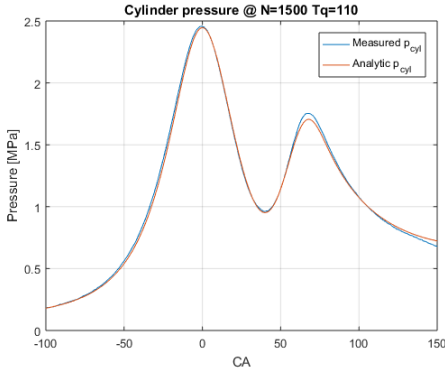


(c) Engine speed  $N = 3000$  RPM, torque  $Tq = 195$  Nm (d) Engine speed  $N = 4000$  RPM, torque  $Tq = 190$  Nm

**Figure 5.9:** MEP before and after the optimization. The blue line is the MEP calculated from the heat release and the red is the tuned MEP to match the desired pressure

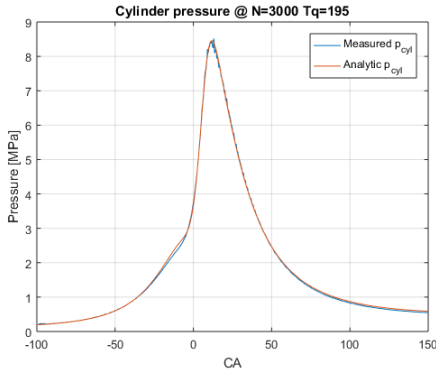
### 5.5.2 Analytical model

As seen in figure 5.10, the model were able to simulate the cylinder pressure with good accuracy for different operation points. The peak pressure for all operations points are in good agreement. In figure 5.11, no major change can be seen in the MFB.

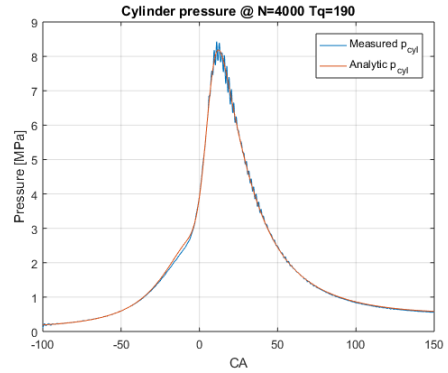


(a) Engine speed  $N = 1500$  RPM, torque  $Tq = 110$  Nm

(b) Engine speed  $N = 2000$  RPM, torque  $Tq = 220$  Nm

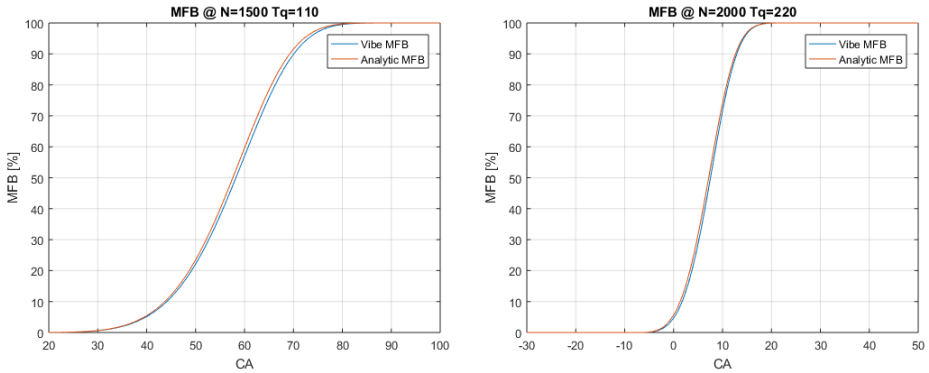


(c) Engine speed  $N = 3000$  RPM, torque  $Tq = 195$  Nm

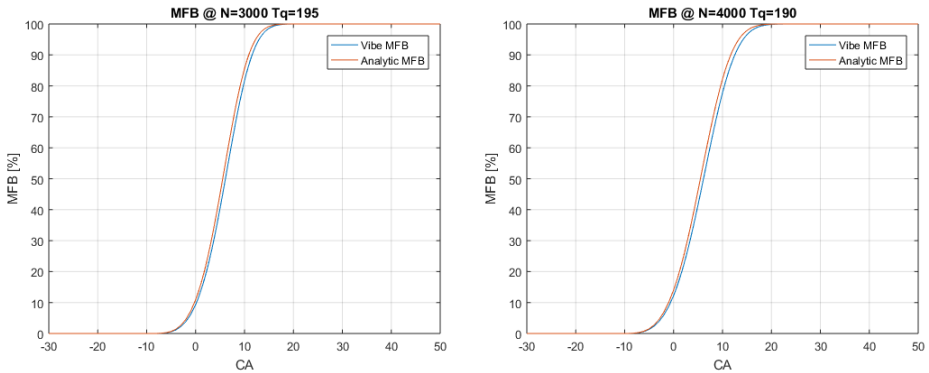


(d) Engine speed  $N = 4000$  RPM, torque  $Tq = 190$  Nm

**Figure 5.10:** Cylinder pressure for different operation cycles



(a) Engine speed  $N = 1500$  RPM, torque  $Tq = 110$  Nm (b) Engine speed  $N = 2000$  RPM, torque  $Tq = 220$  Nm

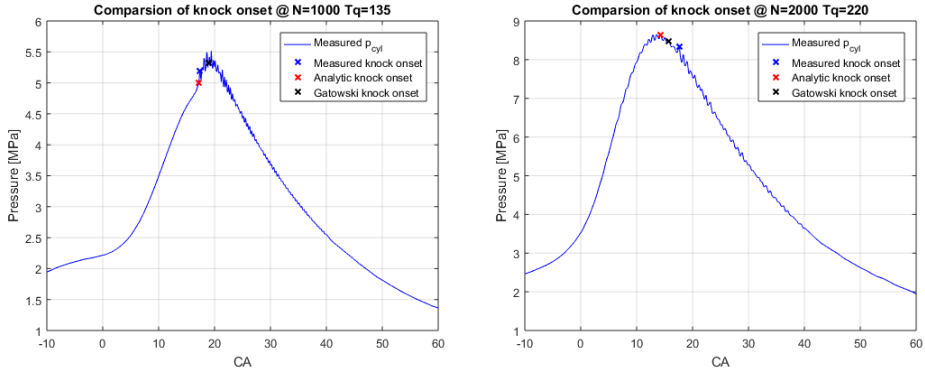


(c) Engine speed  $N = 3000$  RPM, torque  $Tq = 195$  Nm (d) Engine speed  $N = 4000$  RPM, torque  $Tq = 190$  Nm

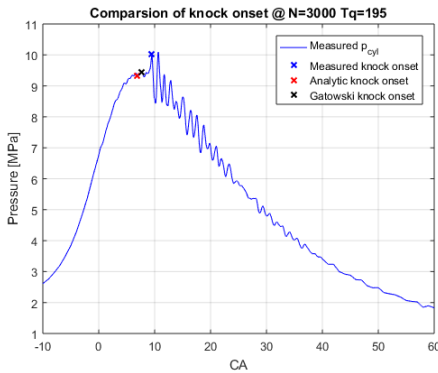
**Figure 5.11:** MFB before and after the optimization. The blue line is the MFB calculated from the heat release and the red is the tuned MFB to match the desired pressure

### 5.5.3 Simulated knock onset for both pressure models

For each operation point the modelled pressure and temperature was implemented in the knock model to validate if the modelled in-cylinder process can be used to predict knock. The validation is done by comparing the measured knock onset with the knock onset predicted with the two different pressure models. To get a better understanding of which model that can predict knock with the best accuracy, a mean average error for several knock cycles is calculated at different operation points. In figure 5.12 the measured pressure curve is the blue line, the blue cross indicates the measured knock onset and the other two crosses indicates the analytic knock onset and the gatowski knock onset.



(a) Engine speed  $N = 1500$  RPM, torque  $Tq = 110$  Nm  
 (b) Engine speed  $N = 2000$  RPM, torque  $Tq = 220$  Nm



(c) Engine speed  $N = 3000$  RPM, torque  $Tq = 195$  Nm

**Figure 5.12:** Shows the pressure curve, the measured knock onset and the modeled knock onset for both pressure models

The error measured in crank angle degree was attained by running the models at fifteen different operation point at 1000, 2000 and 3000 rpm, five for each engine speed. The difference between the measured knock onset and the modelled knock onset was calculated for 20 knocking cycles per operation point and the result can be seen in table 5.5.

**Table 5.5:** The knock onset error for different operation points

N [rpm]	Mean absolute error [deg]		Maximum absolute error [deg]	
	Gatowski	Analytic	Gatowski	Analytic
1000	3.9	1.6	2.2	1.7
2000	2.3	3.9	4.4	6.2
3000	1.9	3.6	3	5

The models seem to have an accuracy within 4 crank angle degrees for the chosen operation points. To choose which model that are best fit to continue to work with the result from previous chapter were taken into account. For predicting knock both models had a similar mean absolute error which leads to comparing the computational time for each model. Since the gatowski model is built on a differential equation and require an *ODE* solver in Matlab, the computational time was way longer for the gatowski model. Therefore, the analytic pressure model was more suitable because the computational time was way shorter and the ability to predict knock was similar to the gatowski model.

The result in figure 5.12 shows that the analytic model detects knock before the measured knock for all three figures. This may due to a poor knock model calibration or an error in the measured knock onset. Since the knock model is calibrated with the measured pressure, the error lies in the pressure model. A perfect pressure model would result in an more accurate model knock onset. Since the accuracy was within 4 crank angle degrees the result is seen as good, but there is always room for improvements.

#### 5.5.4 Polynomial models

The data gathering for the polynomial models were done by simulating the analytic pressure model for all operation points between 1000-4500 rpm. For each operation point, 10 cycles where simulated to minimize the simulation time. Since there is cycle to cycle variation in all SI-engines, average values of the interesting parameters are necessary. The data was evaluated and the relationship between different parameters is presented below. The result that are presented below is at 1000 rpm.

Figure 5.13a shows how the flame development angle change depends on the ignition angle and the intake manifold pressure. Each dot represents an average value for a specific operation point. In figure 5.13b, a second order polynomial was created with equation (5.1) and the Matlab function *lsqnonlin*.

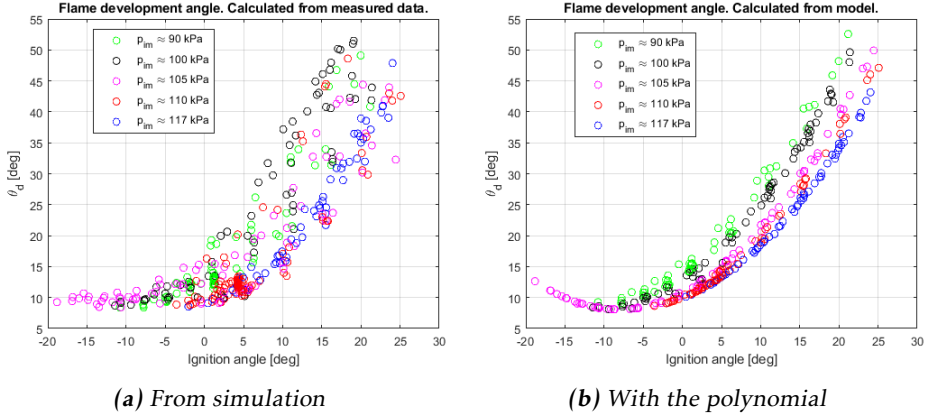


**Figure 5.13:** How the ignition angle and intake manifold pressure change the flame development angle at 1000 rpm.

$$\theta_d = k_1 + k_2 p_{im} + k_3 p_{im}^2 + k_4 \theta_{ign} + k_5 \theta_{ign}^2 + k_6 p_{im} \theta_{ign} \quad (5.1)$$

Figure 5.14a shows how the rapid burn angle change dependent on the ignition angle and the intake manifold pressure. Each dot represents an average value for a specific operation point. In figure 5.14b, a second order polynomial was created with equation (5.2) and the Matlab function *lsqnonlin*.

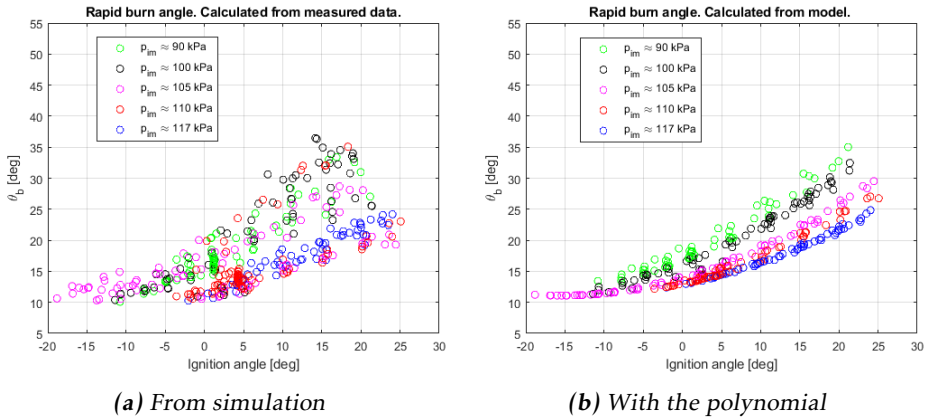
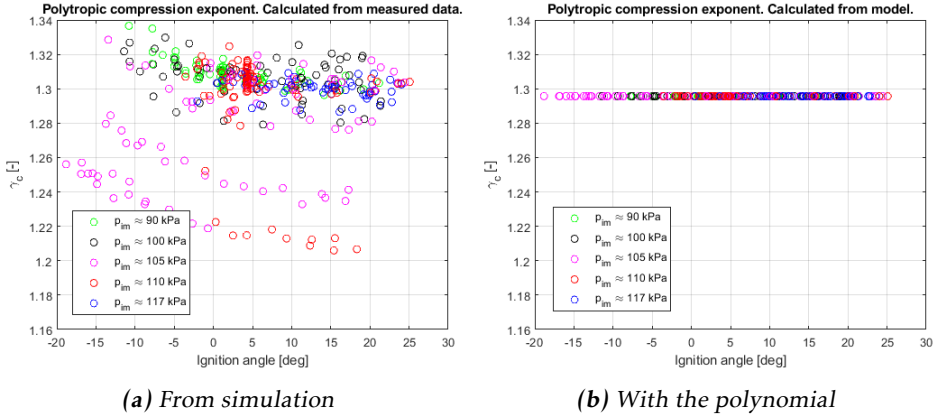


**Figure 5.14:** How the ignition angle and intake manifold pressure change the rapid burn angle at 1000 rpm.

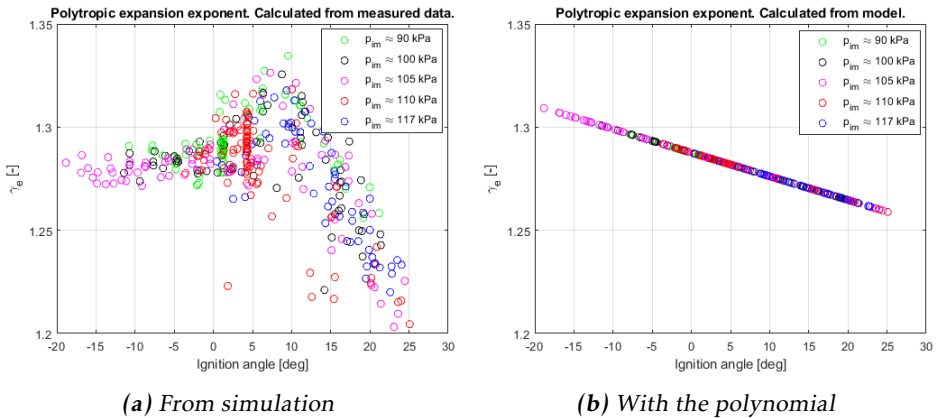
$$\theta_b = l_1 + l_2 p_{im} + l_3 p_{im}^2 + l_4 \theta_{ign} + l_5 \theta_{ign}^2 + l_6 p_{im} \theta_{ign} \quad (5.2)$$

Figure 5.15 and figure 5.16 show the polytropic exponent for the compression and the expansion phase. The figures to the left is values that were gathered from

the simulations and the figures to the right is the created polynomial that were used as one of the polynomial models. The equations for the polynomial can be seen in equation (5.3) and equation (5.4).



**Figure 5.15:** How the ignition angle and intake manifold pressure change polytopric compression exponent at 1000 rpm.



**Figure 5.16:** How the ignition angle and intake manifold pressure change polytopric expansion exponent at 1000 rpm.

$$\gamma_c = n_1 \quad (5.3)$$

$$\gamma_e = m_1 + m_2 \theta_{ign} \quad (5.4)$$

The polynomial for the polytopric compression exponent was modelled as a constant which could result in some error during the compression phase. The reason for this is because no distinct connection was found on the compression

exponent which resulted in the assumption that it was constant for all ignition angles and intake manifold pressures.

Figure 5.17 shows how the ignition efficiency change dependent on the ignition angle and the intake manifold pressure. In figure 5.17b, a second order polynomial was created with equation (5.5) and the Matlab function *lsqnonlin*.

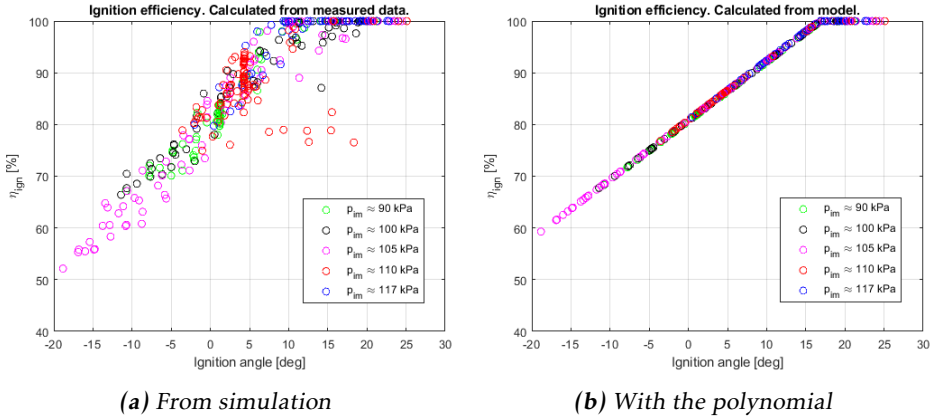


**Figure 5.17:** How the ignition angle and intake manifold pressure change polytropic expansion exponent.

$$\theta_b = b_1 + b_2 p_{im} + b_3 \theta_{ign} \quad (5.5)$$

The values for each parameter in the polynomial expressions in equation (5.1)-(5.5) can be seen the table in appendix A.

### 5.5.5 Pressure validation with the polynomial models

When using the polynomial models and the analytic pressure model, the modelled pressure is validated at different operation points. The model can be seen in figure 5.18. The input parameters are the engine speed, the intake manifold pressure, the variable intake valve timing (VVTi), the ignition angle and the  $\lambda$ -value. The input parameters is sent to the polynomial models where the specific values for the rapid burn angle, flame development angle, ignition efficiency, the polytropic exponent for compression and expansion and the pressure at IVC are found. With these values, the cylinder pressure is modelled with the analytic pressure model.

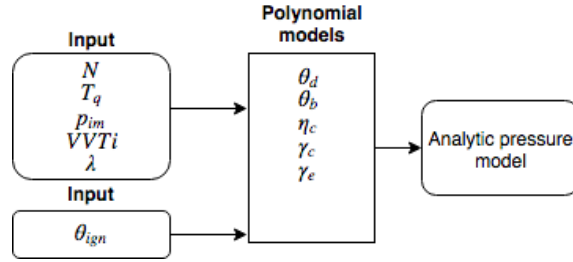


**Figure 5.18:** Show the pressure model with the input signals and the parameters calculated with the polynomial models

In figure 5.19, the measured pressure is compared to the modeled pressure. Each operation point has 50 cycles with different peak pressures due to cycle to cycle variation. Therefore, if the modelled pressure is between the maximum peak pressure and the lowest peak pressure it is assumed to be good.

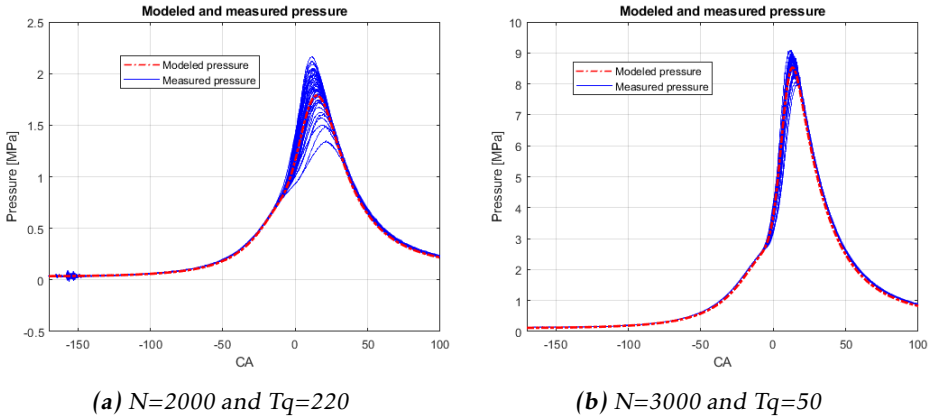


**Figure 5.19:** Shows measured and modeled pressures for two different operation points.

For some operation point, the pressure curve has an offset throughout the hole pressure trace. This can be seen in figure 5.20. In the figure it can be seen that the model starts to differ at IVC and the offset becomes bigger during the compression phase. This shows the importance of having an accurate model for the pressure at IVC since this pressure also affect the Vibe parameters which affect the combustion process.

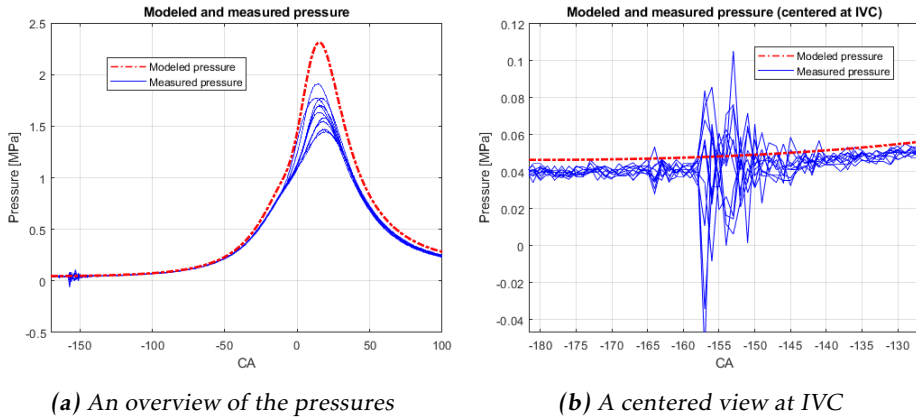


**Figure 5.20:** Shows an operation point where the modeled pressure differs from the measured.

The pressure model was also compared to the validation data from Linköping University. Two plots from the validations can be seen in figure 5.21. As seen in the figure, both of the models are very accurate in the compression and expansion phase. The cycle at 2000 rpm differs a bit during the combustion phase. Although the difference in the combustion phase, the result is rated as good since the model doesn't regard to take cycle to cycle variations.

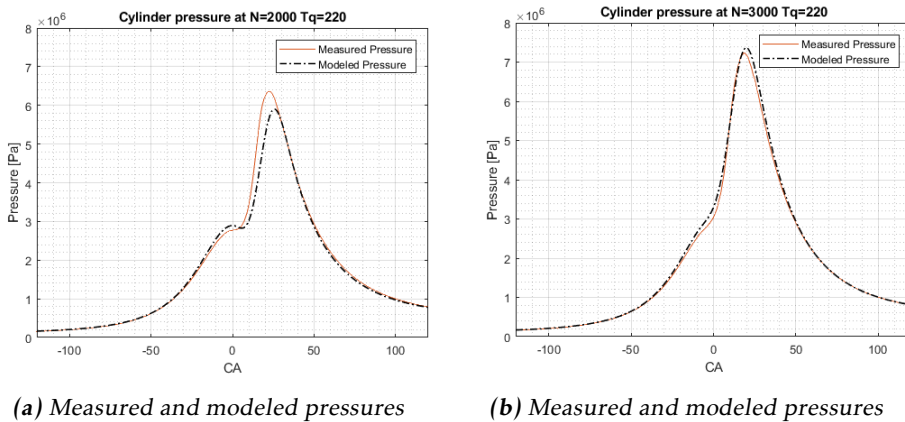


**Figure 5.21:** Shows the modeled and measured pressures from the validation

### 5.5.6 Knock onset validation with polynomial models

The independent pressure model is then connected to the knock model. An overview can be seen in figure 5.22. The model is then validated by comparing the measured knock onset with the knock onset gathered from the model.

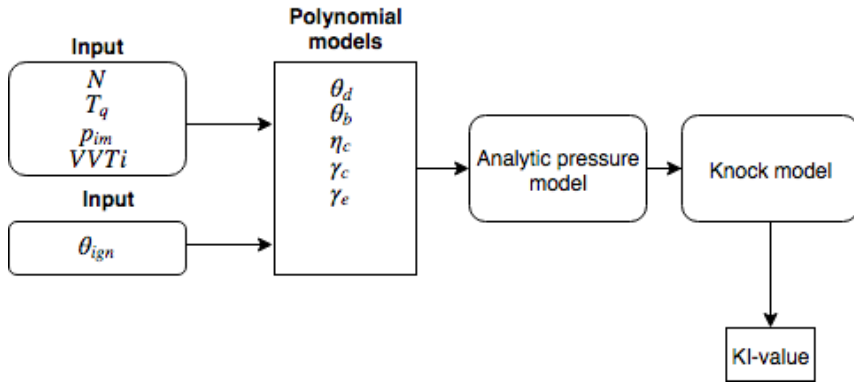


**Figure 5.22:** An overview of the knock onset validation and the sub-models that were used when calculating the knock onset

Figure 5.23, 5.24 and 5.25 shows the modelled pressure compared to the measured pressure for different operation points where knock was detected. Since the ignition angle controller was active during knocking cycles, no exact ignition angle was known, only the average. With the knowledge gathered from section 2.1.1 it is assumed that the cycles with knock are located before the average ignition angle. Therefore, the validation was done by retarding the ignition angle by 1-4 degrees to get a more reliable simulated pressure. In all three figures it is noticed that the modelled pressure is placed between the highest peak and the lowest peak which creates a problem since knock often occur at high pressure. The result of this can be seen in table 5.6, where the minimum, maximum, average and the modelled knock onset is presented for the three operation points. The maximum knock onset will occur for the lower pressure peak and will therefore be closer to the modelled knock onset, which also can be seen in table 5.6.

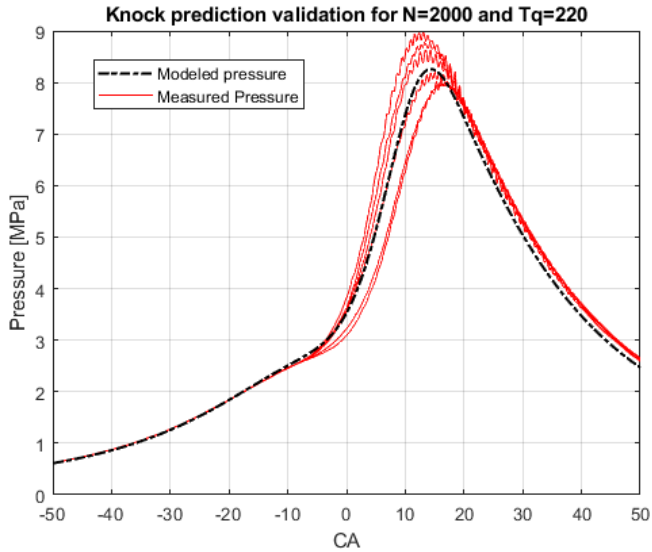


*Figure 5.23: Shows the modelled pressure compared to the measured pressure for a cycle with knock at N=2000 and Torque=220*

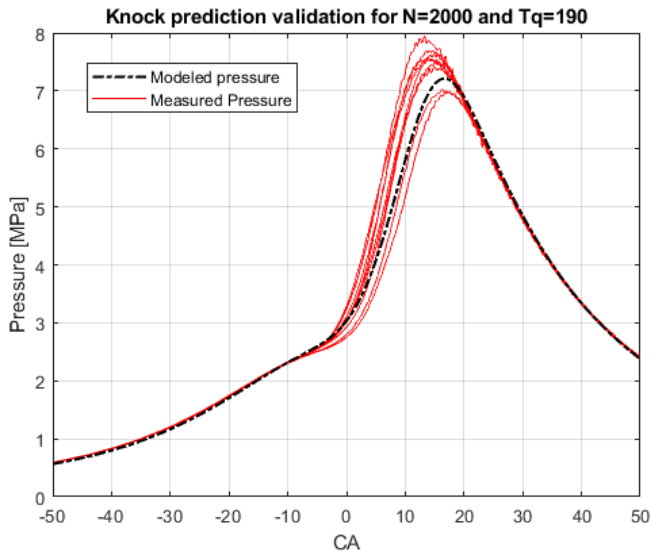


*Figure 5.24: Shows the modelled pressure compared to the measured pressure for a cycle with knock at N=2000 and Torque=190*

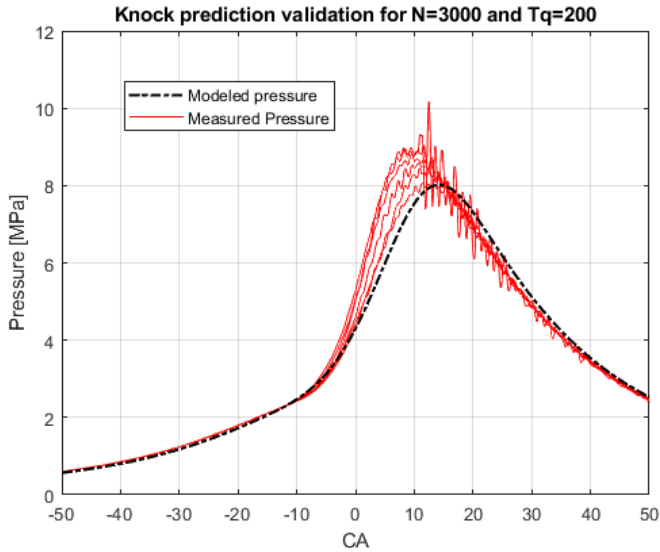


**Figure 5.25:** Shows the modelled pressure compared to the measured pressure for a cycle with knock at  $N=3000$  and Torque=200

**Table 5.6:** The knock onset from the measured pressure and the knock prediction model

Knock onset ATDC [deg]				Difference from average [deg]
Minimum	Maximum	Average	Model	
8	18.5	12.9	18.3	5.3
9	13.5	12.1	18.8	6.7
18.5	19.4	18.9	24.1	5.2

As seen in table 5.6, the knock prediction model have an accuracy within 7 crank angle degrees for the chosen operation points. Unfortunately, there is an uncertainty when judging how good the result is since the ignition angle is unknown for these operation points.

## 5.6 Knock prediction model

The final knock prediction model can be seen in figure 5.26. The modelled cylinder pressure is sent to the knock model that calculates the knock integral. The value of the knock integral will tell if the ignition angle needs to be retarded or advanced according to the algorithm in 3.9.1.

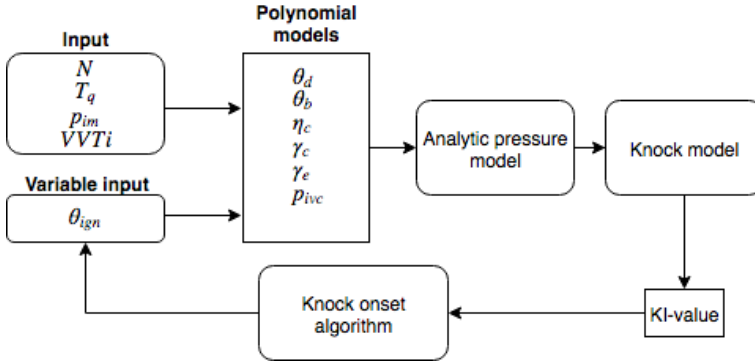


**Figure 5.26:** Show the knock prediction model with the input signals, the parameters calculated with the polynomial models and the important sub-models

### 5.6.1 Knock onset algorithm

To evaluate the knock prediction algorithm, a test were done for 1100 different operation points. The parameters changing for each operation point were the engine speed, the intake manifold pressure, the intake valve closing timing and the lambda value. The results from the test can be seen in figure 5.27.

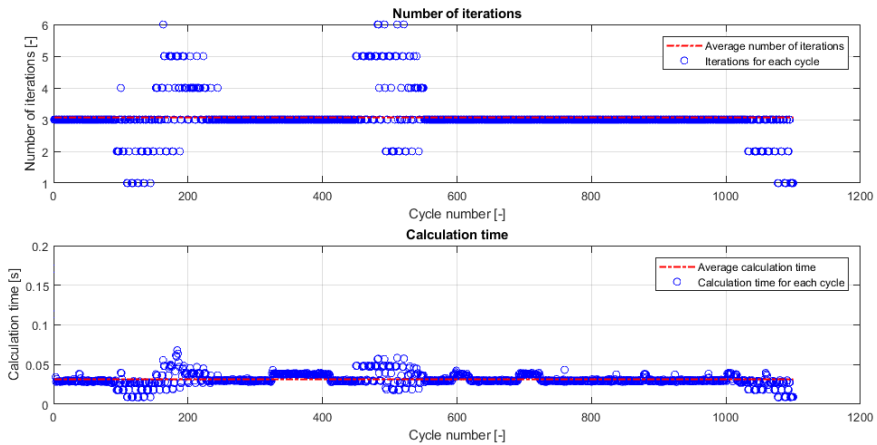


**Figure 5.27:** Shows the number of iterations and calculation time for each operation point. The mean number of iterations were 3.07 and the mean calculation time were 0.032 seconds.

As seen in figure 5.27, some of the cycles only need one or two iteration. For these cycles, the initial first or second guess happened to be the ignition angle that shows knock onset for MFB95.

## 5.7 Discussion

As described in the result, the calculated knock onset with the final model is quite uncertain. The reason for this is mainly because of the amount of sub-models that are used to predict the knock onset. To get a perfect prediction of knock onset, all sub-models needs to be accurate otherwise a propagation of uncertainty will occur. The prediction can be improved by changing the modelling strategy for the following tasks:

**Polynomial models:** As seen in the results, the extended model with the polynomial model will differ a bit from the regular analytic model, even though they have the same input variables. The reason for this may be the lack of accuracy for the polynomial model. This could be improved by adding more input parameters and increasing the grades of the polynomials.

**Knock Integral:** As seen in the results, the tuned knock integral is in good agreement while testing on the measured pressure, within 4 degrees. When testing it with the simulated analytic pressure, it differs a bit more and the mean difference is at 3.03 degrees. When the analytic pressure model was extended with the polynomial models it started to differ a lot more. The mean difference is now above 5 degrees. The main reason for this is because the extended pressure model does not take cycle to cycle variations into account. The simulated pressure will therefore be an average of the pressure traces from the measured data. The mean knock onset will therefore be delayed since knock will occur more often in random high peaks than in random low peaks. To avoid this problem, some compensation for the cycle to cycle variations should be added to ether the knock integral or the extended pressure model.



# 6

---

## Conclusion

The main goal of this thesis was to investigate if a physical based model could be used to predict knock onset. The model strategy was to compare two different pressure models and based on the performance, choose one to continue creating a polynomial that expressed the combustion parameters that were used later in the final knock prediction model. The result showed that an analytic pressure model could recreate a measured pressure curve with great accuracy. After tuning the knock model with the measured data, the pressure model could determine if knock would occur within 4 crank angle degrees which was seen as a good result.

The combustion parameters can be expressed with polynomial expressions, but some parameters were too simplified which led to some errors in the final model. Also, when making a polynomial expressions for the combustion parameters, it is important to understand that the cycle to cycle phenomena is neglected which creates a big uncertainty when validating the knock onset. Therefore, the knock prediction model showed poor results because the modelled pressure was an average out of 50 cycles. The result of this was that the modelled knock onset was, in the best case, off by 5-7 crank angle degrees compared to the measured knock onset. In the worst case, when there was an error in the pressure already at IVC as seen in figure 5.20, the knock model could indicate that knock would occur even tho there was no knock in that operation point.

Although, the result showed that there is a possibility to make a more accurate knock prediction model. If each sub-model is more accurate, for example if the pressure model was more focused on the peak pressure, the result would be significantly improved.

## 6.1 Future work

To improve the knock prediction model there are some areas that would simplify the modelling process.

1. First, a complete set of measured data, i.e not an average out of 50 cycles, for parameters such as ignition angle, intake manifold pressure, exhaust manifold pressure,  $\lambda$ -value etc.
2. Improving the knock onset detection. The presented method of detecting knock onset worked between 1000-3000 rpm. At higher engine speed the noise was too large and the pressure oscillation limit was hard to determine using a Matlab script. To set the knock onset manually would work, but that would take too much time and it is a very inefficient way of doing the modelling. Therefore, a better method of detecting the knock onset would increase the opportunity for a wider model.
3. Improving the coefficient in the knock integral. Some kind of adaptive coefficient that changes its value depending on engine speed, ignition angle etc. would be interesting to investigate.
4. Instead of using the knock integral to determine if there will be knock, one could investigate the relationship between the unburned temperature and the knock onset. Since the knock integral is heavily dependent on the unburned temperature, which is a function of the cylinder pressure. A simplification of the knock integral would be interesting to investigate, where the unburned temperature is the only parameter that is required to determine if knock will occur.
5. Expand the polynomial expressions so the combustion parameters can be expressed with more parameters. This would result in less chance of errors when choosing the parameters at a specific operation condition.

# Appendix



# A

## Polynomial values

*Table A.1: The polynomial parameters at different engine speeds*

Parameter	Engine speed [rpm]					
	1000	2000	3000	3500	4000	4500
$k_1$	225	563	80.12	48.92	57.63	73.07
$k_2$	-2.88e-5	-0.5	-0.0423	0.0312	0.047	-0.022
$k_3$	0.01	1.3e-4	9.20e-4	1.94e-4	5.647e-4	6.316e-4
$k_4$	-4.74	-11	-1.875	-1.12	-1.307	-1.667
$k_5$	0.004	0.058	0.0141	0.0094	0.011	0.012
$k_6$	-0.024	0.0049	-0.0020	-0.0016	-0.0024	-0.0016
$l_1$	50	167	1.19e+2	64.77	1.0924e+2	1.239e+2
$l_2$	-0.5	-0.17	0.360	0.958	-0.0561	-0.230
$l_3$	0.0085	9.91e-4	0.00186	-0.002	0.0032	0.0028
$l_4$	-0.321	-3.34	-3.085	-2.155	-2.392	-2.740
$l_5$	0.012	0.204	0.026	0.021	0.0211	0.022
$l_6$	-0.015	-0.001	-0.0097	-0.0094	-0.0080	-0.0048
$m_1$	1.402	1.475	1.29	1.349	1.317	1.297
$m_2$	-0.001	-0.002	-3.51e-4	-0.001	-6.704e-04	-4.513e-4
$n_1$	1.296	1.40	1.42	1.377	1.419	1.432
$b_1$	-0.35	-0.107	-0.134	0.026	0.0060	0.042
$b_2$	1.45e-4	4.91e-4	-2.70e-4	-5.915e-4	-0.0015	-6.794e-4
$b_3$	0.011	0.0095	0.0108	0.0098	0.0108	0.010



---

## Bibliography

- [1] Alasdair Cairns and Hugh Blaxill. The effects of combined internal and external exhaust gas recirculation on gasoline controlled auto-ignition. *SAE Technical Paper*, 2005. doi:10.4271/2005-01-0133. Cited on page 9.
- [2] Jinseok Chang, Manshik Kim, and Kyoungdoug Min. Detection of misfire and knock in spark ignition engines by wavelet transform of engine block vibration signals. *INSTITUTE OF PHYSICS PUBLISHING*, 2002. Cited on page 6.
- [3] Christel Elmqvist, Fredrik Lindström, Hans-Erik Ångström, Börje Grandin, and Gautam Kalghatgi. Optimizing engine concepts by using a simple model of knock prediction. *SAE Technical Paper*, 2003. doi:10.4271/2003-01-3123. Cited on pages 8, 12, 15, and 32.
- [4] Lars Eriksson. Spark advance modeling and control. *PhD thesis, Linköping Universitet*, 1999. Cited on pages 5, 6, 7, and 15.
- [5] Lars Eriksson and Ingemar Andersson. An analytic model for cylinder pressure in a four stroke si engine. *SAE Technical Paper*, 2002. doi:10.4271/2002-01-0371. Cited on pages 7 and 20.
- [6] Lars Eriksson and Lars Nielsen. *Modeling and Control of Engines and Drivelines*. John Wiley and Sons Ltd, first edition, 2014. Cited on pages 8, 15, 17, 18, and 21.
- [7] Lars Eriksson and Martin Sivertsson. Computing optimal heat release rates in combustion engines. *SAE Technical Paper*, 2015. doi:10.4271/2015-01-0882. Cited on page 18.
- [8] Lars Eriksson and Martin Sivertsson. Calculation of optimal heat release rates under constrained conditions. *SAE Technical Paper*, 2016. doi:10.4271/2016-01-0812. Cited on pages 8 and 12.
- [9] G.D Errico, T. Lucchini, A. Onorati, M. Mehl, T. Faravelli, Ranzim E., S. Merola, and B. M. Vaglieco. Development and experimental validation of a combustion model with detailed chemistry for knock predictions. *SAE Technical Paper*, 2007. doi:10.4271/2007-01-0938. Cited on page 8.

- [10] J.A. Gatowski, E.N. Balles, K.M. Chun, F.E. Nelson, Ekcia J.A., and J.B. Heywood. Heat release analysis of engine pressure data. *SAE Technical Paper*, 1984. doi:10.4271/2015-01-0882. Cited on page 18.
- [11] A. Gogan, B. Sundén, L. Montorsi, S. S. Ahmedand, and F. Mauss. Knock modeling: An integrated tool for detailed chemistry and engine cycle simulation. *Journal of Dynamic Systems, Measurement and Control*, 1976. Cited on page 8.
- [12] John Heywood. *Internal Combustion Engine Fundamentals*. McGraw Hill, Inc, 1988. Cited on pages 5, 7, 8, 12, 14, and 21.
- [13] Bjoerne Hoepke, Stefan Jannsen, Emmanuel Kasseris, and Wai K. Cheng. Egr effects on boosted si engine operation and knock integral correlation. *SAE Technical Paper*, 2012. doi:10.4271/2012-01-0707. Cited on page 8.
- [14] M. Hubbard, P. D. Dobson, and J. D. Powell. Closed loop control of spark advance using a cylinder pressure sensor. *SAE Technical Paper*, 2003. doi:10.4271/2000-01-0932. Cited on page 7.
- [15] Sung-Hwan Hwang Jong-Hwa Lee and Yong-Seok Cho Jin-Soo Lim, Dong-Chan Jeon. A new knock-detection method using cylinder pressure, block vibration and sound pressure signals from a si engine. *SAE Technical Paper*, 1998. doi:10.4271/981436. Cited on page 5.
- [16] Uwe Kiencke and Lars Nielsen. *Automotive Control Systems, For Engine, Driveline, and Vehicle*. Springer Verlag, 2nd ed. edition, 2005. Cited on page 7.
- [17] Masao Kinoshita, Akinori Saito, Kazuhisa Mogi, and Kouichi Nakata. Study on ion current and pressure behavior with knocking in engine cylinder. *JSAE Technical Paper*, 2000. doi:10.1016/S0389-4304(00)00069-2. Cited on page 6.
- [18] Rani Kiwan, Anna G. Stefanopoulou, Jason Martz, Gopichandra Surnilla, Imtiaz Ali, and Daniel Joseph Styl. Effects of differential pressure measurement characteristics on low pressure-egr estimation error in si-engines. *IFAC-Papers*, 2016. doi:10.1016/j.ifacol.2016.08.105. Cited on page 8.
- [19] Markus Klein. Single-zone cylinder pressure modeling and estimation for heat release analysis of si engines. *PhD thesis, Linköping Universitet*, 2007. Cited on page 18.
- [20] U Lezium, M Schultalber, W Drewlow, and B Lampe. Improvements in knock control. *Univeristy Of Rostock/Institut of Automotion*, 2007. Cited on page 5.
- [21] Toru Noda, Kazuya Hasegawa, Masaaki Kubo, and Teruyuki Itoh. Development of transient knock prediction technique by using a zero-dimensional simulation with chemical kinetics. *SAE Technical Paper*, 2004. doi:10.4271/2004-01-0618. Cited on page 8.

- 
- [22] David Scholl, Terry Barash, Stephen Russ, and William Stockhausen. Spectrogram analysis of accelerometer-based spark knock detection waveforms. *SAE Technical Paper*, 1997. doi:10.4271/972020. Cited on page 6.
- [23] Andreas Thomasson, Lars Eriksson, Tobias Lindell, James C. Peyton Jones, Jill Spelina, and Jesse Frey. Tuning and experimental evaluation of a likelihood-based engine knock controller. *52nd IEEE Conf. on Decision Control*, 2013. Cited on page 7.
- [24] Andreas Thomasson, Haoyun Shi, Tobias Lindell, Lars Eriksson, Tielong Shen, and James C. Peyton Jones. Experimental validation of a likelihood-based stochastic knock controller. *SAE Technical Paper*, 2016. Cited on page 7.
- [25] I Vibe. *Brennverlauf und Kreisprozess von Verbrennungsmotoren*. Verlag Technik Berlin, 1970. Cited on page 8.
- [26] Yeliana, Christopher Cooney, Jeremy Worm, and Jeffrey.D Naber. The calculation of mass fraction burn of ethanol-gasoline blended fuels using single and two-zone models. *SAE Technical Paper*, 2008. doi:10.4271/2008-01-0320. Cited on page 7.
- [27] Guoming G. Zhu, Chao F. Daniels, and James Winkelman. Mbt timing detection and its closed-loop control using in- cylinder pressure signal. *SAE Technical Paper*, 2003. doi:10.4271/2003-01-3266. Cited on page 7.